LA-UR- **98-3857**

Approved for public release; distribution is unlimited.

Title: **Residual stress measurement by successive extension of a slot: The crack compliance method**

Author(s): **Michael B. Prime**

Submitted to: **Applied Mechanics Reviews**

Vol. 52, No. 2
pp. 75-96
1999

Los Alamos
NATIONAL LABORATORY

Residual stress measurement by successive extension of a slot: The crack compliance method

Michael B. Prime

Engineering Sciences and Applications Division, MS P946
Los Alamos National Laboratory, Los Alamos, NM, 87545 prime@lanl.gov

This article reviews the technical literature on the determination of a residual stress profile by successive extension of a slot and measurement of the resulting strains or displacements. This technique is known variously in the literature as the crack compliance method, the successive cracking method, the slotting method, and a "fracture mechanics based approach." The article briefly summarizes the chronological development of this method and then, to facilitate more detailed review, defines the components that make up the method. The theory section of the article first considers forward method solutions including fracture mechanics, finite element, analytical, and body force methods. Then it examines inverse solutions, including incremental inverses and series expansions. Next, the article reviews all experimental applications of the crack compliance method. Aspects reviewed include the specimen geometry and material, the details of making the slot, the deformation measurement, and the theoretical solutions used to solve for stress. Finally, the article makes a brief qualitative comparison between crack compliance and other residual stress measurement methods. In many situations, the crack compliance method offers several advantages over other methods: improved resolution of residual stress variation with depth; the ability to measure both small and very large parts; measurement of stress intensity factor caused by residual stress; measurement of crack closure stresses; increased sensitivity over other material removal methods; and the ability to measure non-crystalline materials. This review article contains 77 references.

1 INTRODUCTION

Residual stresses play a critical role in failures due to fatigue, creep, wear, stress corrosion cracking, fracture, buckling, and more. Additionally, residual stresses often cause dimensional instability, such as distortion after heat treating or after machining a part. Residual stresses are those present in a part that is free of external loads, and they are generated by virtually all manufacturing processes. They add to applied loads and are particularly insidious because they satisfy equilibrium and, therefore, offer no external evidence of their existence.

Because of the major contribution of residual stresses to failures and their almost universal presence, knowledge of residual stresses is crucial for any engineering structure where liberal safety factors are impractical. Ideally one would like to accurately predict or model residual stresses resulting from the various manufacturing operations. A great deal of research effort is focused on this task. However, the problem is very complex. Development of residual stress generally involves nonlinear material behavior and often involves material removal, phase transformations, and coupled mechanical and thermal problems. For the majority of problems, the current predictive capabilities are insufficient to give adequate knowledge of residual stresses. So, the ability to measure residual stress is critical for two purposes: (1) to minimize residual-stress related failures, and (2) to aid in developing predictive capabilities by verifying models.

A semantic note is in order at this point. Some researchers object to the phrase "measuring" residual stress, noting correctly that one measures strain or displacement and then "determines" residual stress. In this article, "measure" and "determine" are used interchangeably. The reader is assumed capable of making the distinction if necessary.

This literature review is limited to a specific subset of the residual stress literature [1-52]. The techniques reviewed here measure residual stress variation with depth by incrementally introducing a slot or cut into a part containing residual stress. Depth here refers to the direction of slot extension. Some measure of deformation, such as strain or displacement, is taken at each increment of depth. From these measurements, the residual stress profile that originally existed in the part is calculated.

Usually, only the normal stress component normal to the slot face is determined. A discussion of the effect of shear stresses on these measurements is postponed to Section 2.4, after a set of coordinates and some terminology have been defined.

Other techniques that use a slot but fall outside the scope of this review include the cutting of two deep slots on either side of a strain gauge to measure uniform stress near

the surface [68,74], the determination of axial (longitudinal) residual stress in a solid rod from a single measurement of opening of a longitudinal slit [53,63,65], the measurement of residual hoop stress in plastic pipes by assuming a linear variation and then slitting through a ring [57], and the measurement of growth stresses in logs (timber) by measurement of saw cut opening [54].

One might prefer to measure residual stress nondestructively. However, there are crucial gaps in the capabilities of nondestructive techniques (Lu et al. [62]). The two primary nondestructive techniques are x-ray diffraction (XRD) and neutron diffraction (ND). XRD can nondestructively measure residual stress in crystalline materials to a maximum depth of about 0.05 mm. Measuring to a greater depth requires layer removal, such as by etching, and makes the measurements destructive. ND can measure residual stress to depths of many centimeters but is generally constrained to measuring a volume no smaller than a cube 1 to 2 mm on a side. This constraint makes it difficult or impossible to resolve residual stress variations over distances of less than about 1 mm. Furthermore, ND cannot measure stresses much deeper than about 50 mm for engineering materials. Therefore, considering ND and XRD, nondestructive measurement is not feasible over the large range from 0.05 mm to 1 mm and for depths greater than about 50 mm. Unfortunately, residual stresses that vary over this range are produced by many of the most common manufacturing processes: heat treating, machining, forging, cladding, and casting, for example. At the same time, the primary contribution of residual stress to mechanical failures, such as from fatigue and fracture, can occur over the 0.05 mm to 1 mm range.

Additionally, there are other limitations to the XRD and ND methods:

(1) Sensitivity to grain size and texturing effects. Crystalline structural anisotropy may render the measured residual strains to be ambiguously related to the actual macroscopic residual stress.

(2) Complete inability to measure non-crystalline materials.

(3) Difficulty measuring stresses on curved surfaces for XRD. The path length of the scattered beam is increased, which cannot be distinguished from strain, leading to errors.

(4) A typical stress depth profile obtained using XRD or ND methods may take days to a week. The same stress profile using crack compliance could be accomplished in one day.

These limitations illustrate the need for residual stress measurement techniques that fill in the missing capabilities of current methods.

A good source for information on the many other residual stress measurement methods is Lu et al. [62], although its coverage of the work reviewed here is very poor. Cheng and Finnie [17] summarized their own work on the crack compliance method.

2 BACKGROUND & TERMINOLOGY

Techniques for measurement of residual stress using successive extension of a slot are known in the technical literature by several names: crack compliance method, fracture mechanics approach, successive cracking method, slotting method, rectilinear groove method, etc. In this paper, the term originally coined by Cheng and Finnie [2], the crack compliance method or compliance for short, is used as an inclusive term. The name came from the similarity of this technique to the compliance method for measuring crack length in a fatigue or fracture specimen [70]; a known load was applied to a cracked specimen, and the resulting strain was used to determine the crack length. In the residual-stress crack compliance method, the crack length is known and the measured strain is used to calculate the residual stress.

2.1 Historical Overview

Although it does not meet the criteria of this review, Schwaighofer's [74] early work (1964) deserves mention as the first use a slot to measure residual stress. He machined two slots in a part and determined the surface residual stress using strain measurements taken between the slots. He recognized that the subsurface stress variation would affect the measurement but did not postulate the possibility of using successive slot extensions to measure the variation. The measurement of strain at incremental depths to measure a residual stress profile was introduced for hole drilling measurements by Soete and VanCrombrugge [75] and Kelsey [60], although their implementations were theoretically incorrect.

What is here termed the crack compliance method was originally introduced by Vaidyanathan and Finnie in 1971 [52]. They measured residual stress in a butt-welded plate by introducing a hole in the plate and then extending a slot from the hole using a jeweler's saw. At each increment of slot length, they measured the stress intensity factor, K_I, using a cumbersome photoelastic technique. Then they inverted a solution for K_I to get a closed form solution for residual stress from the variation of K_I. The method appeared to successfully measure the residual stress, although there was little with which to compare the results.

This method saw minimal use in the following years. The experimental difficulty in performing the photoelasticity measurements likely discouraged others from applying Vaidyanathan and Finnie's idea. The original work also relied on a closed form solution for K_I for a crack subjected to arbitrary loading on the crack faces. Such solutions were not available for many practical configurations.

By the mid 1980s, technological advances stimulated new research using the crack compliance method. This new research is evidenced by publications from researchers in several countries: Cheng and Finnie (1985 [2]) from the United States, Ritchie and Leggatt (1987 [44]) from the Netherlands and the United Kingdom, Fett (1987 [19]) from Germany, Reid (1988 [42]) from the United Kingdom, and

Kang, Song, and Earmme (1989 [29]) from South Korea. Computational advances had made it both possible and relatively simple to solve the solid mechanics problems necessary for application of the compliance method for arbitrary geometries. These computational techniques also allowed the residual stresses to be calculated from measured strains or displacements, instead of from K_I. This approach allowed the much more convenient and universally available strain gauges to replace photoelastic measurements. Since these early publications, the technique has seen many advances and new applications.

Special note should be made of the driving force behind the development of the crack compliance method, Professor Iain Finnie of the University of California, Berkeley. Although he never appears as the lead author, he invented the method [52], and has been instrumental in its development [2-18, 22,38,45,48,49].

2.2 Components of Method

The compliance method can be broken down into several distinct components, common to all applications of the method. They include analytical, experimental, and application differences. There are tradeoffs between the accuracy, precision, and ease of implementation of the various possibilities. These choices and tradeoffs will be the focus of this literature review.

There are generally two components to the analytical portion of the compliance method: the forward and inverse solutions. The forward solution is the answer to the question "What are the strains (or displacements, or K_Is) that would be measured if one incrementally introduced a slot into a part with an arbitrary, known residual stress distribution?". These strains as a function of slot depth are referred to as the *compliance functions* or *compliances*. This question can generally be answered using fracture mechanics solutions, the finite element method, or other numerical techniques. The inverse solution is then the answer to the question "What original residual stress distribution best matches the strains that were actually measured?". This question can be answered by using the forward solution and then solving for the average residual stress at each increment of depth sequentially, or by using more sophisticated inverse solutions such as series expansions. This choice will substantially influence both the accuracy and the depth resolution of the measurement results.

There are also several experimental choices to be made when applying the crack compliance method. The first choice is how to introduce the slot. Possibilities include saws, milling cutters, and electric discharge machining. The choice may depend on the particular application. For example, cutters tend to break when cutting into a compressive stress field. The next choice is how to measure the resulting deformations. Strain gauges may be used, and a decision must be made on where to place them and how many to use. Another possibility is displacements measured with a clip gauge, moiré interferometry, or a micrometer.

There are many distinctions among the applications of the crack compliance method found in the literature. Materials tested include metals, polymers, and composites. Geometrical configurations which have been tested include surface and through thickness measurements, axisymmetric stresses in cylindrical bodies, pre-cracked specimens, central holes, and more.

2.3 Terminology and Definitions

Figure 1 defines a coordinate system for rectangular coordinates and some common terms. In the crack compliance method, a *slot* or *cut* is introduced into the part. A *crack* would be a *slot* of zero width. The slot starts from the *top face* or *surface* of the part and is extended in the *x*-direction towards the *back face*. The two surfaces normal to the *z*-direction are the *edges*. The *y*-direction is normal to the slot. The normal stress component measured by such a slot is σ_y. Stress variation with *depth* means variation in the *x*-direction, and the *slot depth* is called *a*. The *thickness* of the part, *t*, is its dimension in the *x*-direction at the plane of the crack. The *remaining* or *uncracked ligament* is the intact portion of the part in the crack plane, given by $a < x < t$. The opening of the crack or slot at the *surface* is called the *crack opening displacement* or *COD*. For a slot of finite width, the *COD* is generally the total opening minus the undeformed slot width.

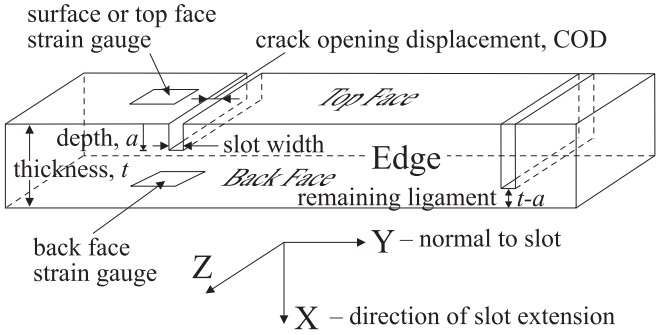

Figure 1. Coordinate system and terminology.

Figure 2 shows some additional definitions and terms for cylindrical geometries. The figure shows the two types of cuts made to measure residual stresses, both shown for convenience starting from the outer surface although they may start from the inner surface. Both cuts are extended incrementally in the radial direction, so they are identified by the other coordinate in the cut plane. A *circumferential cut* wraps around the entire part circumference. It releases *axial* stress, which is normal to the cut plane. An *axial cut* extends along the axial length of the part and releases the *hoop* or *θ stress*. Some researchers refer to this cut as a *radial cut* instead of axial. Researchers measure either axial or hoop strains.

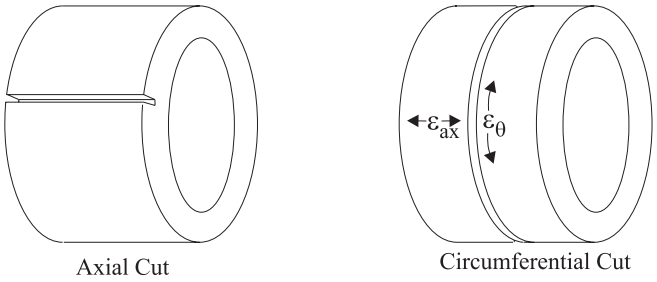

Figure 2. Slots in cylindrical geometries.

2.4 Normal and Shear Stress Components

The literature covered in this review only reports crack compliance measurements of the stress normal to the face of the slot, σ_y in Figure 1. However, the slot will also release two shear stress components, τ_{yz} and τ_{xy}. Such shear strain, if present at the slot location, could affect the strains measured after extending the slot and, hence, the determination of σ_y. There are several reasons why this is usually not a practical concern for crack compliance measurements.

The shear stress in the plane of the surface of the part, τ_{yz}, is measured by other methods such as hole drilling. There is little discussion of this shear stress in the crack compliance literature, but two simple arguments can explain why it has little effect on crack compliance measurements as compared with hole drilling.

First, by geometrical considerations, this shear stress component will have only a small effect on the *y*-strain measured by the surface strain gauge. In fact, Cheng et al. [8] discuss determining τ_{yz} by measuring the surface shear strain, γ_{yz}, rather than normal strain. At a material point, normal strains are only affected by normal stresses at that material point. For the surface strain gauge, this relation is $\varepsilon_y = (\sigma_y - \nu\sigma_z)/E$. The local shear stress only affects the shear strain, $\gamma_{yz} = \tau_{yz}/G$. Releasing shear stresses at the slot location has only a small effect on normal stresses at typical strain gauge locations. Because the hole-drilling method uses a strain gauge rosette and measures at least one normal strain at an angle to the *y* and *z* axes, the shear stress does have a direct effect on the strain measurement. This can be seen by considering a Mohr's circle transformation to get the normal stresses in the direction of strain measurement.

Second, by the free surface condition, τ_{yz} must be zero on the edges of the part. These stresses are not likely to build to a significant value unless the part is large in the *z*-direction at the location of the slot. Since hole drilling is easily applied well away from an edge, the same argument does not apply.

The *x*-*y* component of shear stress is more often discussed in the crack compliance literature. However, it also has little effect on most measurements. By the free surface condition, this shear stress must be zero on the top face where the slot is initiated. For this reason, it is assumed to be negligible for near surface measurements using either crack compliance or hole drilling. For through-thickness residual stress measurements, τ_{xy} cannot be assumed negligible. However, Cheng and Finnie [11] showed that this component of residual shear stress has no effect on the *y*-strains measured on the back face directly opposite the slot. This is the location most commonly used in the literature for through-thickness measurements.

3 REVIEW—THEORY

This section reviews papers that introduce or develop theoretical considerations for either the forward or inverse problems. As discussed in 2.2, the forward problem calculates what stresses would be measured for a given stress distribution. The inverse problem uses results from the forward solution to determine a stress distribution that "best" matches the experimentally measured deformations. This forward and inverse type of approach is generally necessary because a direct calculation of residual stresses from measured deformation is not possible. This review covers a few exceptions, which generally involve substantial approximations.

3.1 Forward Solutions

Researchers use fracture mechanics solutions, finite element methods, or other numerical methods to arrive at forward solutions or "compliances," as defined in 2.2. A wide variety of geometries have been considered, leading to a convenient grouping distinguishing between solutions in rectangular and cylindrical coordinates. The solutions are generally for linearly elastic, isotropic materials. Many solutions treat the slot as a mathematical crack. A few include the finite width of the machined slot.

Almost all of the work reviewed here uses a simplifying superposition principle to solve the forward problem. At first, the problem sounds daunting. When a slot or crack is introduced into a part containing residual stresses, some stresses are released and the general stress distribution is rearranged. At each increment of depth, the rearrangement is superimposed on the results from the previous step. How does one tractably calculate the deformations? Bueckner's superposition principle [55], originally developed for fracture mechanics, is employed. This principle, illustrated in Figure 3, says that the deformations can be calculated by considering the cracked body and loading the crack faces with the residual stresses that originally existed on this plane in the *uncracked* body.

It is possible to make a forward solution without using this superposition principle. For example, Perl and Aroné [37] simulate residual stresses in a finite element model with thermal loads and then remove material to calculate deformations. As another approach, finite element software often allows one to specify residual stress as an initial condition and then to remove elements to simulate material removal. With that approach, care must be taken to ensure that the model does not give strains because the initial residual stress state does not satisfy equilibrium. The first step in the finite element analysis should allow the body to achieve equilibrium. The state after this step should be

considered the undeformed shape, and subsequent analysis steps can simulate cutting the slot.

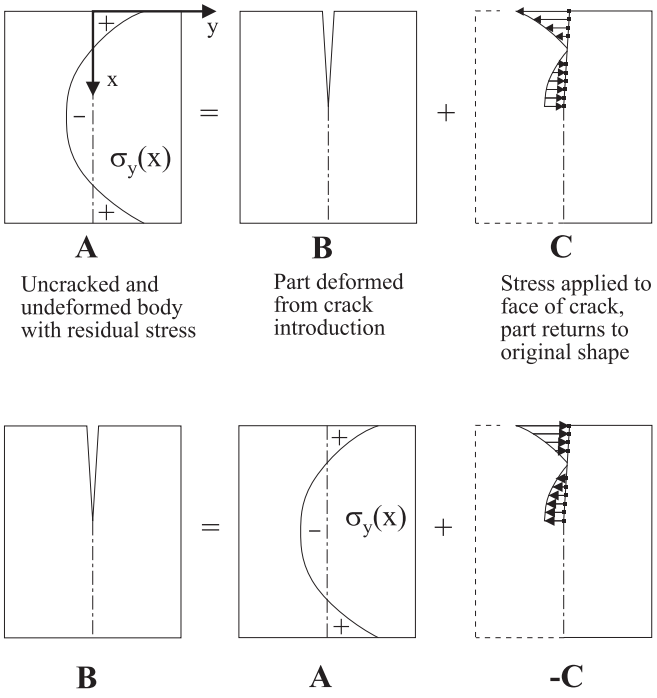

Figure 3. Superposition principle used to calculate deformations from releasing residual stresses.

Which method should one use to calculate a new forward solution? For a single test, a finite element solution may be the quickest, and a strategically constructed mesh that allows easy simulation of the slot cutting by removing elements or constraints will save much effort. The research reviewed in this article indicates that there is no need for special mesh refinement at the crack tip. For multiple tests on similar geometries, programming one of the fracture mechanics, body force, or other numerical solutions could easily save time in the long run. For a new geometry, an existing solution may be a sufficiently close approximation. In addition to the solutions reviewed in this article, compendiums of fracture-mechanics weight function solutions are available [59,76]. The application of weight function solutions to crack compliance measurements is discussed in this chapter. If no solution for a similar geometry is available or the geometry is complex, a finite element solution may be appropriate. For near surface measurements where the width and shape of the slot become important, a finite element solution may again be the best choice.

Unless otherwise noted, the solutions presented in this section require numerical solution. It should also be made clear that all K_I solutions are for a mathematical crack, not a finite width slot. In addition to describing the solution, the review explicitly states whether the solution gives strains or displacements.

3.1.1 Cartesian Coordinates

This section presents solutions for deformations due to stresses in rectangular (x,y,z) coordinates. For near-surface stresses in polar coordinates, for example σ_θ near the surface of a cylinder, the stresses can be treated as rectangular if the region examined is small compared to the radius of curvature. Figure 4 shows the various geometries referred to in this section. Solutions for surface stresses consider a crack or slot in the free surface of a semi-infinite body. This configuration is also often referred to as a single edge notched strip. Solutions for through-thickness geometries include the effect of the back face. Solutions are also reviewed for a crack in the interior of an infinite plate and for a crack starting from an interior hole.

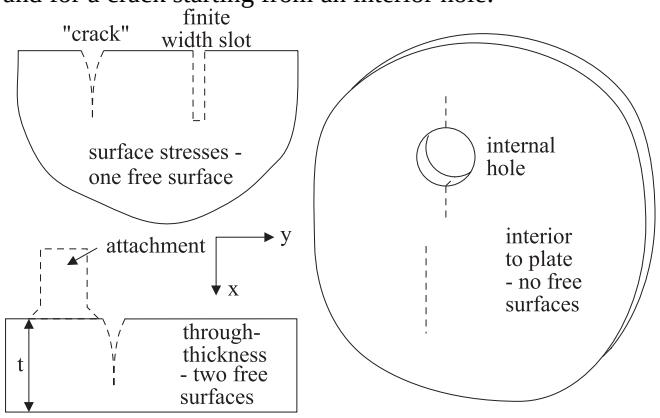

Figure 4. Geometries for rectangular coordinate forward solutions.

In the first appearance of the crack compliance method, Vaidyanathan and Finnie [52] used a K_I solution for a crack in the interior of a plate. It was a weight function solution, which allows K_I to be calculated in integral form for arbitrary loading on the crack:

$$K_I(a) = \int_0^a \sigma(y) h(y,a) dy ,$$

where h is the weight function. Because they were measuring K_I directly, using photoelasticity, the solution calculated only K_I because of the release of residual stresses, rather than strains or displacements.

Fett [19,20] calculated the crack opening displacement for a near-surface stress measurement using an existing weight function K_I solution. Kang et al. [29] also calculated compliances for a single edge notched strip using a different weight function solution for the same geometry. They calculated surface displacements using Castigliano's theorem and a virtual force at the location of strain measurement.

Cheng and Finnie developed a set of solutions specifically for crack compliance measurements of normal and shear stress through the thickness of a strip. They claimed that previous weight function solutions were in error for the limiting a/t values less than 0.05 or near 1. They presented a K_I solution, constructed from other solutions accurate for limited ranges of a/t, that they claimed to be accurate for all values of a/t [5]. Cheng and Finnie [6] repeated this solution for K_{II}, which could be

used for measuring *x-y* shear stresses using crack compliance. Then Cheng et al. [10,11] applied both of these solutions to calculate displacements and strains.

Ritchie and Leggatt [44] used the finite element method (FEM) to calculate compliances for a slot sawed through the thickness of a strip. The geometry modeled was a 2-D slot including the actual slot width and considering all deformations to be plane stress. Successive elements were removed from the finite element mesh to allow calculations for different slot depths. Strain was calculated on the top and bottom surfaces of the strip, as well as on the edge. Beghini and Bertini [1] performed a similar calculation, also using 2-D plane stress finite elements.

Finnie et al. [22] used a 2-D finite element analysis to calculate compliances for the case when the part width (in the *z*-direction) varied. The specimen had a clad layer that was thinner in the *z*-direction than the substrate. They also used a strength of materials approach to correct for out of plane bending caused by high compressive stresses.

Several investigators have developed forward solutions for through-thickness measurements on a compact tension specimens. Reid [42] calculated a closed form approximation. Although he derived the inverse solution directly (see 3.2.4), it can be shown to be equivalent to the forward solution described here. He used a simple beam bending approximation, Figure 5. The uncracked ligament was conceptually separated from the cracked portion of the compact tension specimen. The residual stress distribution was used to calculate an equivalent force and moment to be applied to the beam. Simple beam theory then gave back face strains. Prime [40] demonstrated that this approximation resulted in unacceptably large errors and developed a more accurate forward solution using Schindler's technique [46,49] and a weight function solution by Fett and Munz [59].

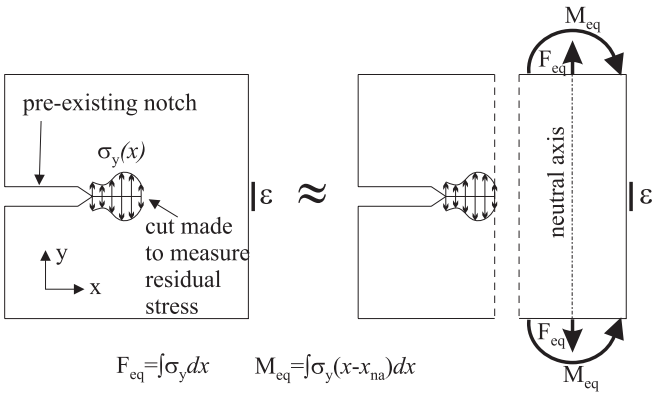

Figure 5. Reid [42] approximation for compact tension specimen using equivalent force and moment.

Cheng et al. [8] presented a solution for measuring near-surface residual stresses for strains measured very near the cut. They considered both normal stress loading, σ_y, and out-of-plane shear stress, τ_{yz}, using K_I and K_{III} solutions, respectively. They calculated displacements using Castigliano's theorem and then differentiated to get strain. The solution was claimed to be valid to a final depth of $a/t < 0.05$. They also estimated that the crack length in the out-of-plane direction, *z*, needed to only measure 8 times the final depth of cut for their 2-D solution to give accurate results for a 3-D experiment. Therefore, one does not have make the slot through the whole *z* width of a large part. Schindler presented a very simple to implement weight function solution for strains measured near a surface cut [49].

Cheng and Finnie [13] presented the first non-FEM solution for the compliances for a slot of finite (non-zero) width. They considered a rectangular slot in a semi-infinite plane under residual stress loading from both normal stress, σ_y, and shear stress, τ_{xy}. The calculations were performed using Nisitani's body force method [64], which uses the point force solution for an uncracked body. These point forces are applied along the prospective slot boundary, and their magnitudes are adjusted numerically to satisfy the appropriate boundary conditions. The calculations indicated that, for slots with a depth of less than 5 times the slot width, significant errors will results from approximating the slot as a crack. Cheng et al. [15] gave a simple correction for a slot with a semi-circular bottom, such as that produced using wire electric discharge machining.

Lai et al. [31] investigated residual stresses near a hole in a plate. They considered the introduction of cracks symmetrically on opposite sides of the hole and calculated the resulting displacements. They used a fracture mechanics approach and the weight function for a crack emanating from a center hole.

Cheng and Finnie [14] presented a solution for measuring through thickness residual stresses near an attachment to a plate (see Figure 4). They gave a bracket welded to a nuclear reactor pressure vessel as an example of this configuration. The attachment could be of arbitrary geometry and have elastic constants different from the plate. They combined a fracture mechanics solution for an edge-cracked strip with finite element calculations for the effect of the bracket. Strain at the back face was the quantity calculated. They performed calculations on trial configurations and found that the errors from ignoring the presence of the attachment could exceed 10%.

Prime and Finnie [38] presented a solution for compliances for a finite width slot in layered material. They considered a surface layer on a semi-infinite substrate with different elastic constants, and the slot could penetrate into the substrate. They used the body force method, basically the same approach as Cheng and Finnie [13]. The presence of the substrate significantly affected the compliances for a slot penetrating halfway through the layer when the elastic moduli differ by 50 percent or more.

Nowell et al. [34] calculated compliance functions for a through-thickness crack with a dislocation density analysis. At each depth, the crack is modeled by a continuous distribution of displacement discontinuities, or dislocations. The prescribed crack-face tractions result in an integral equation for the dislocation density, which is

solved numerically. From the density variation, one can calculate strain at any location in the body.

3.1.2 Cylindrical Coordinates

This section examines forward solutions in cylindrical coordinates. It should be noted that, for measuring near-surface stresses in a cylindrical geometry, it is possible to use a surface stress solution in rectangular coordinates if the region considered is small compared to the radius of curvature. A word of caution is also in order. Some of the solutions presented are only accurate away from the immediate region of the cut. So they may not be applicable for data from a strain gauge very near the slot.

Cheng and Finnie [2] calculated compliances in a thin-walled cylinder for the case of axisymmetric axial residual stresses. They considered a circumferential crack starting at the cylinder's inner surface and hoop strain measured on the outer surface. They also mentioned the possibility of using strains measured on the inner surface for a crack starting from the outer surface. Strain was calculated with a K_I solution for arbitrary loading on the crack faces. Cheng and Finnie [4] revisited this solution and gave compliances in tabular form.

Cheng and Finnie [3] calculated compliances in a thin-walled cylinder for the case of axisymmetric hoop residual stresses. They considered an axial crack, starting at the outer surface. Hoop strain on the outer surface was calculated with a K_I solution for arbitrary loading on the crack faces. The solution was valid for strain gauges located at least the wall thickness away from the cut. Cheng and Finnie [7] added corrections to the previous solution for the case of thick-walled cylinders. Kang and Seol [30] also calculated compliances for a thick-walled cylinder. They calculated hoop strains on the outer surface with a weight function solution.

Perl and Aroné [37] calculated compliances for a thick-walled cylinder with a particular residual stress distribution. In an autofrettaged cylinder, internal pressure has been applied to cause yielding and subsequent residual stresses. The authors considered an array of 7 equally spaced axial cuts starting from the cylinder inner surface and calculated compliances using finite elements with the residual stresses simulated by a thermal load. The calculated deformation was hoop strain on the inner surface between adjacent cuts.

Schindler [45,46,49] calculated compliances for a solid disk with an axial crack. He calculated surface hoop strains with a weight function solution and gave procedures to ensure accuracy for near-surface or very deep cracks, where weight function solutions may be in error. Fett and Thun [21] also calculated compliances for a solid disk with an axial crack using a weight function and additionally included a solution for a central, internal crack. Their solutions were formulated to give crack opening displacement.

3.2 Inverse Solutions

This section reviews the methodology researchers use to invert from measured deformations as a function of slot depth to the originally existing residual stresses. Most of these techniques use one of the forward solutions described in the previous section. The forward solution gives the deformations that would be measured for a given stress distribution. The inverse solution then gives a stress distribution that in some way results in the "best" correlation with the actual measurements. A comparison, which could be relevant for crack compliance, of inversion techniques for the incremental hole-drilling method is given by Schajer [72].

Note that the inverse solution pioneered by Schindler [46,49] and discussed in 3.2.2 reveals not only the residual stress profile but also the stress intensity factor that would be present for a crack growing in the part. In fact, the solution gives the stress intensity factor first and with a very simple calculation.

The only direct comparison of inversion techniques is given by Prime [40], who simulated a compact tension specimen preloaded beyond yield using finite elements. He simulated various errors in the strain measurements and applied the Legendre series expansion inverse [2] and Schindler's incremental inverse [46,49]. Both methods were shown to be quite error tolerant if implemented carefully. Gremaud et al. [25] also demonstrated that the series expansion inverse is quite tolerant of zero-shift and random errors in the strain measurements.

3.2.1 Inherent Limits on Inversion

There are inherent limits on inverting from the measured strains to the residual stress profile. These limits apply to all inversion methods, and crack compliance method practitioners must be aware of them. There are two main limits, and they are inter-related.

First, the spatial resolution is inherently limited by the distance between the strain measurement and the location of the desired interior stresses. To resolve stress variations over a distance of say 1 mm, you must make cuts with increments of less than 1 mm. However, just making cuts in finer depth increments is not necessarily sufficient. The strain changes resulting from each cut must be measurable and significant. A more distant strain gauge will generally give smaller strain changes for a given cut and, therefore, decrease the spatial resolution. Note that because of geometric effects this is not a function of distance only. For example, a back face strain measurement can resolve stresses better than a closer surface gauge for some cut depths.

Second, the stability and uniqueness of the inverse must be considered. For measurements with a top surface gauge, the inverse will become unstable at some depth. Physically this occurs because the surface gauge will eventually respond quite weakly to the release of sub-surface stresses. The depth at which the inversion is unstable is not well defined for crack compliance measurements, but Cheng et al. [8] indicate that one can

determine stresses to a depth of at least 1.0 to 1.2 times the distance from the edge of the cut to the center of the strain gauge. Schajer [72] extensively discussed this issue for hole-drilling, and presumably a similar analysis could be applied to crack compliance. For hole drilling, the maximum depth is given as about 0.3 to 0.4 times the mean radius of the strain gauge rosette, which corresponds to about 0.4 to 0.7 times the distance from the edge of the hole to the center of the strain gauges. For hole drilling, this depth limit can be extended by using a larger strain gauge rosette and a larger hole. This will result in a corresponding decrease in spatial resolution. For crack-compliance, there is usually room for multiple gauges at different distances from the slot. This can increase the maximum depth while sacrificing spatial resolution only for the deeper portion of the measurements.

3.2.2 Incremental Stress

Many crack compliance method investigators, beginning with Ritchie and Leggatt [44], calculate residual stresses in a step-by-step manner. They determine an equivalent stress for each increment of slot depth, based on the strain reading in that increment and the stresses from previous increments. This is the oldest and still most common method for obtaining a stress profile, often used with hole drilling. We will call this the *incremental stress* method.

We must make an important note about correctly using an incremental stress inverse. This method was originally developed for use with the hole drilling method. Early implementations had significant theoretical errors, as discussed by Schajer [72]. For example, Kelsey [60] assumed that the change in strain measured after an increment in hole depth was only affected by the stress released in that depth increment. However, the geometrical change of extending the hole would change the strain even if there were no stresses released in that depth increment. The incremental stress approach described here, combined with correct use of the forward solutions described in Section 3.1, is theoretically sound. It appears that all crack compliance literature in this review has correctly implemented the incremental stress approach. However, because of the lack of detail in some papers, one cannot be certain.

In its simplest form, the incremental stress technique suffers from several drawbacks. Crack compliance method researchers employ various techniques to counter these potential shortcomings. To facilitate this review, a description of this technique in its simplest form is given. Then the major drawbacks are described. Following that, the variations on the incremental stress used by crack compliance researchers are described.

Incremental Stress - Basic Implementation

At each of the m increments of slot depth, the resulting deformation at some location is measured. Here strain is considered, although the measurement may be of displacement:

$$\varepsilon_1, \varepsilon_2, .. \varepsilon_m \ .$$

In the end, the average residual stress in each increment is calculated:

$$\sigma_1, \sigma_2, .. \sigma_m \ .$$

One must realize that the strain measured at each increment of cut is a function of the current depth and the stress not only in that increment but also in all previous increments:

$$\varepsilon_1 = f(\sigma_1, a_1), \varepsilon_2 = f(\sigma_1, \sigma_2, a_2) ..., \varepsilon_m = f(\sigma_1, \sigma_2, ..., \sigma_m, a_m).$$

The stress in the first increment is calculated by considering the forward solution for a uniform stress of 1 in the first increment. Using linear superposition, the actual magnitude of stress in the first increment is given:

$$\sigma_1 = \frac{\varepsilon_1}{\varepsilon(\sigma_1 = 1, a = a_1)}. \qquad (1)$$

For subsequent increments, additional calculations are necessary. The strain after the second cut depends on the stresses in both of the first two increments and the new geometry. So the portion of strain due to the stress in the second increment only must be calculated by subtracting off the strain due to the first increment stress and the new slot length,

$$\varepsilon_2'(\sigma_2, a_2) = \varepsilon_2(\sigma_1, \sigma_2, a_2) - \varepsilon_2''(\sigma_1, a_2), \qquad (2)$$

where ε_2 is the actual measured strain after the second cut, and ε_2'' is the strain that would be measured after the second cut due to the stress in the first increment only. Then the stress in the second increment can be calculated using the forward solution for a uniform stress of 1 in the second increment only:

$$\sigma_2 = \frac{\varepsilon_2'}{\varepsilon(\sigma_2 = 1, a = a_2)}. \qquad (3)$$

This procedure is repeated for subsequent increments. The stress calculated in each increment will be a function of the calculated stress in all previous increments. Using this procedure, the calculated stress distribution *exactly* reproduces the measured strains.

As presented here in its simplest form, this inversion technique suffers from three main potential drawbacks:

1. Error Accumulation/Propagation

Because the stress calculated in each increment depends on the stresses calculated in each previous increment, errors will accumulate. The error in the stress measured in the first increment will add approximately linearly to that measured in the second. The stress in the third increment will then contain compound effects of the errors in the first two intervals, and so on. Unfortunately, the first increment is generally the most prone to errors because it has the lowest strain reading. However, because of the physical constraints of the problem, there is a self-correcting effect. Therefore, the resulting stress profile may be quite noisy, but it will not monotonically diverge in one direction from the actual profile.

2. Measurement Error Intolerance

Because the number of known strains and unknown stresses are equal, the calculated stress distribution will exactly match the measurements. Because the experimental measurements virtually always contain errors, this is generally not a desirable feature as it ensures errors in the stress distribution.

3. Error - Resolution Tradeoff

The two error types mentioned above can be reduced by taking larger increments of cut depth. However, this results in decreased spatial resolution of the stress distribution. So one must sacrifice accuracy for resolution or vice versa.

Incremental Stress Applied to Crack compliance

The applications of the incremental stress approach to crack compliance all appear to use uniform increments of slot depth. This can result in increasing errors because, for a given increment, the sensitivity decreases with increasing depth. It is possible to use non-uniform depth increments to minimize the sensitivity to errors in the strain measurements. For example, Zuccarello [77] determined optimal depth increments for the ring core method.

Ritchie and Leggatt [44] combined the incremental stress approach with a least squares fit to minimize errors. Strains were measured at *k* distinct locations for each of the *m* slot depths. A least squares fit was performed to give the *m* σ_i that best reproduced the *k* x *m* measured strains. Note that it would be possible to perform the least squares fit at each increment sequentially. However, the authors combined all *m* increments into a single fit in order to minimize error propagation. Note also that this least squares approach requires multiple deformation measurements at each depth.

Kang et al. [29] supplemented the incremental stress method with data smoothing. They fitted second order polynomials to successive sets of 7 data points using least squares. They also used stress increments of 3 times the cutting increment, 3Δa, in reducing the data for their preferred compromise between resolution and accuracy. This also provided redundant data and allowed a least squares fit. Kang and Seol [30] averaged the readings of two strain gauges on opposite sides of the crack and then smoothed the data.

Beghini and Bertini [1] developed an approach with one more unknown than the number of depth increments, a least squares fit, and additional constraints. They considered a residual stress distribution that varied linearly within each of the *m* increments. Considering continuity, this was characterized by a single stress value at *m* + 1 nodes. Readings from strain gauges at multiple locations allowed a least squares fit to find the *m* + 1 nodal stresses that best reproduced the measurements. Because the authors measured residual stress through the thickness of a cross section, they added the constraints that the stress distribution satisfy force and moment equilibrium. Note that this approach, which gives a non-uniform stress in each increment, shares some characteristics with the series expansion approaches described in 3.2.3.

Schindler [46,49] developed a unique inversion technique that first provides the mode I stress intensity factor caused by a crack extending in the residual stress field and then provides the residual stress profile. He showed that K_I could be determined using

$$K_{Irs}(a) = \frac{E'}{Z(a)} \frac{d\varepsilon}{da}, \tag{4}$$

where *Z(a)* is the influence function, which depends on the geometry and the location of the strain measurement but *not* on the residual stress distribution, and *E'* is *E* for plane stress and $E/(1-\nu^2)$ for plane strain. Schindler gives *Z(a)* for a variety of configurations [45-51], and given *Z* the calculation in Eq. 4 is very simple to implement. However, because this approach requires differentiation of experimental data, increased errors are possible. Prime [40] applied this approach to data with simulated noise and errors and showed that the effect is small for differentiation using a smoothing technique, such as a four-point smoothing differential or a smoothing spline fit. The residual stress profile is calculated from $K_I(a)$ using an incremental inverse based on a weight function solution for K_I. Many of the existing weight function solutions [59,76] are inaccurate for deep cracks. Schindler [73] discusses the calculation of accurate weight functions for deep cracks.

3.2.3 Series Expansion

The second common inverse solution is to solve for the stress variation expressed as a series expansion. This approach was pioneered for residual stress measurement method by Schajer [71] for hole drilling and Popelar et al. [69] for a sectioning method. It was first applied to the crack compliance method by Cheng and Finnie [2] and Fett [19]. As in the previous section, a general description of the approach will be followed by descriptions of its application to crack compliance problems.

Series Expansion - Basic Implementation

Assume that the unknown stress variation as a function of depth can be expressed as a series expansion,

$$\sigma_y(x) = \sum_{i=1}^{n} A_i P_i(x) = [P]\{A\}, \tag{5}$$

where the P_i are some functional series, such as polynomials, *x* is generally normalized by the final cut depth, and the A_i represent unknown coefficients to be solved for. Using a forward solution, the strains that *would* be measured for each term in the series are calculated. These are called the compliance functions C_i. Using superposition, the strains given by the series expansion can now be written as

$$\varepsilon_y(x) = \sum_{i=1}^{n} A_i C_i(x) = [C]\{A\}. \tag{6}$$

A least squares fit is performed to minimize the error between the strains given by Eq. 6 and the *m* strain

measurements. This gives the A_i and can be written in matrix form as

$$\{A\} = \left([C]^T [C]\right)^{-1} [C]^T \{\varepsilon_{measured}\}. \quad (7)$$

Now the stress distribution is given by Eq. 5.

As with the incremental stress method, there are several potential drawbacks to this method.

1. Convergence

It is generally hoped that as the order of the expansion, *n*, increases, the result will converge to a solution. But after some point, the fit will diverge. This necessitates some method for selecting an appropriate fit order.

2. Ability of Expansion to Fit Actual Distribution

The accuracy of the solution is dependent on the ability of the chosen series expansion to fit the actual distribution within a convergent number of terms in the series. If the actual stresses vary too rapidly or in some other way are not expressible in terms of the chosen expansion, errors will result.

3. Endpoint Stability

Series expansions of this type using polynomials often exhibit instability near the endpoints of the fitted range. This can often be observed by comparing results for successive even and odd expansions, *n* and *n+1* in Eq. 5. So the stresses given by this technique may be less accurate at the surface and the final cut depth.

Series Expansion Applied to Crack compliance

Legendre polynomials are commonly used with the series expansion approach because the higher order terms automatically satisfy equilibrium. Cheng and Finnie [2] expressed axisymmetric axial residual stresses through the thickness of a cylinder with Legendre polynomials. By excluding the 0th order (uniform stress) term, the resulting stresses are guaranteed to satisfy axial equilibrium. They used three terms in the series to fit strain data from eight cut depths and several strain gauges and noted that calculations using a power series instead of Legendre polynomials resulted in a less convergent fit. Cheng and Finnie [7] noted that, for measuring through-thickness longitudinal stresses in a plate, excluding the 0th and 1st order terms guarantees the satisfaction of stress and moment equilibrium. The highest order Legendre expansion appearing in the literature is $n = 9$ by Cheng et al. [12,14]. Cheng and Finnie [14] averaged between successive orders of the series expansion (i.e., 8th and 9th), presumably to minimize endpoint instability.

Power series expansion are commonly used for near-surface measurements. Fett [19,20] expressed stresses partially through a bar with a 5th degree power series expansion. Cheng et al. [8] also discussed measuring stresses near the surface using a power series expansion.

Researchers occasionally constrain the solution to match a symmetry inherent to the problem by using a subset of a series. Fett and Thun [21], using the symmetry when measuring axisymmetric hoop stresses through the thickness of a solid disk, used only even terms in a power series expansion. Cheng and Finnie [18] used only even Legendre polynomials to order 6 for the measurement of axisymmetric through-thickness hoop stresses in a solid rods to ensure both symmetry and zero slope of the stresses at $r = 0$.

Fett [19,20] suggested a Fourier expansion instead of polynomials if the stress distribution is expected to have a discontinuity. However, such a solution may be slow to converge. Gremaud et al. [24], Finnie et al. [22], and Prime and Hellwig [39] used two separate polynomial expansions to get stresses in a clad layer and the underlying substrate, there being an allowable discontinuity across the interface.

Nowell et al. [34] expressed stresses through the thickness of a beam with a Fourier series instead of polynomials. No reasons were given. However, a Fourier series may be less susceptible than polynomials to endpoint instability

For a stress field that cannot be accurately fit with continuous polynomials, Gremaud et al. [25] proposed a spline-based alternative they called “overlapping piecewise functions.” They divided the region of stress variation into a set of overlapping intervals. Then the stress in each interval was expressed as a linearly or quadratically varying series expansion using a least squares fit. The intervals were fit sequentially, with the effect from each previous interval considered as with the incremental stress method. An averaging procedure gave continuity at the region of overlap between successive intervals. This technique is more computationally intensive than a continuous series expansion but promises to combine the best features of the series expansion and incremental stress methods. It was also applied by Prime and Hellwig [39].

3.2.4 Miscellaneous Inverse Methods

Vaidyanathan and Finnie [52] were able to use a closed form inverse because of their unique experimental methods and choice of specimen configuration. First, they measured K_I directly, rather than strain or displacement, using a photoelastic coating. Second, they considered a slot interior to a plate. For a crack of length *2a* cut into a residual stress field symmetric about the center of the crack, $x = 0$, the weight function solution can be solved for the stresses:

$$\sigma_y(a) = \frac{1}{\sqrt{\pi}} \frac{d}{da} \int_0^a \frac{K_I(x)\sqrt{x}}{\sqrt{a^2 - x^2}} dx \,. \quad (8)$$

Presumably this equation was solved numerically from measurements of K_I at the discrete cut lengths. This closed form inverse required direct measurement of K_I, here using a cumbersome photoelastic technique, and was limited to a crack internal to a plate.

Joerms [28] used an approximate finite element method to solve for the stresses from displacement measurements after introducing an axial saw cut into a railroad wheel. In this case, the stresses and the wheel thickness varied in the out-of-plane direction, *z*, as well as in the depth direction. He interpolated measured displacements to get displacement values throughout the surface of the cut. Then he modeled the final state of the wheel after the saw cut and forced the displacements back

to the uncut state. He claimed that the resulting stress distribution may not be unique, but it could exist and would satisfy the boundary conditions.

Reid [42] used a beam bending approximation to calculate residual stresses in a compact tension specimen from strains measured during extension of the notch. As discussed in 3.1.1 and illustrated in Figure 5, he calculated the equivalent force and moment due to releasing residual stresses and applied them to the uncracked ligament. The result was a closed form integral equation for residual stresses in terms of the measured strains. Prime [40] demonstrated that this approximation resulted in large errors.

Read [41] measured the *J*-integral resulting from residual stresses for a semi-elliptical surface crack of successive depths. Strain gauges were placed along a contour around the crack. By approximating some terms in the contour integral and then numerically integrating, *J* was given as a function of depth.

Perl and Aroné [37] inverted from measured strains to the autofrettage level in a cylinder. Their forward solution indicated that the strains measured when their set of axial cuts penetrated 7.5% to 15% through the thickness of the cylinder wall were especially indicative of autofrettage level. A simple formula was given to calculate autofrettage level from these strains. Perl [66] extended this technique to a single cut. However, he now only takes strain readings after the cut completely separates the ring rather than at incremental cut depths, which removes the work from the scope of this review.

Orkisz and Skrzat [36] outlined a technique to reconstruct residual stresses from measurements taken during successive extension of an axial slot in a railroad wheel. For such a part, both geometry and residual stresses vary in the out-of-plane, *z*, direction as well as the depth direction, *x*, increasing complexity significantly. They proposed to use strain measurements, crack opening displacements, and Moiré interferometry. The inverse solution for residual stress was to be accomplished using constrained optimization methods. This is applied first to a solution for the plastic zone, the region in the wheel where irreversible strains occurred. From the plastic zone solution, a solution in the surrounding elastic zone would be similarly obtained. This technique was not applied to either an actual or simulated experiment.

3.3 Other Considerations

A common question asked of crack compliance researchers is “does the shape of the slot matter?”. Many of the forward solutions consider the slot as a mathematically sharp crack, whereas a saw cut will have a square profile, an EDM cut will have a semi-circular bottom, and one can sharpen a crack tip to get a V-notch [29]. Cheng and Finnie [13] compared square-bottomed slots with mathematical cracks and concluded that, for elastic behavior, a slot could be considered a crack without significant errors (> ~10%) when the depth was more than five times the width. For the best results when making this approximation, use the distance from the nearest edge of the slot to the strain gauge as the crack-to-gauge distance for the analysis. Slot shapes other than square-bottomed could be expected to behave similarly. So the answer to the original question is that the shape of the slot only matters for near-surface measurements where the slot’s depth to width ratio is less than about five. For near-surface measurements, Cheng et al. [15] gave a simple correction to a solution for a square-bottomed slot [13] for the case of an EDM slot with a semi-circular bottom. When one considers plasticity effects, Petrucci and Zuccarelo [67] mentioned that the profile of the slot, especially the sharpness of the corners, can make a difference. Their study only considers square-bottomed slots, so no quantitative conclusions can be made about the relative effect for different shapes. It seems reasonable to assume that yielding effects would be lowest for a semi-circular bottomed slot, where there are no sharp corners.

Very little research has evaluated the effect of yielding on residual stress measurements using the crack compliance method. Petrucci and Zuccarello [67] investigated plasticity effects for a residual stress measurement technique where one cuts grooves on both sides of a strain gauge and determines a uniform stress from a single strain reading for a deep slot. They used a plane-stress finite-element analysis with elastic-perfectly plastic behavior and the Von Mises yielding criterion. They found the errors to be negligible for residual stresses below half the yield stress and to depend on the slot depth for higher residual stresses. One would expect the errors to be even lower for a strain hardening material. The implication of these results is not apparent for the crack compliance method, where a residual stress profile is determined using successive depths of a single slot. Schindler and Finnie [48] made a correction for local yielding effect in tests on a Charpy specimen. They assumed a yielded region in front of the crack tip, calculated the expected results for such a case, and fit their measurements to this case.

4 REVIEW — APPLICATIONS

This section reviews all known experimental applications of the crack compliance method. Computational or simulated experiments are excluded.

The configuration of the application drives many of the experimental choices, such as type of cutting, type and location of deformation measurement, and forward and inverse solutions. For this reason, applications in rectangular and cylindrical coordinates are considered separately. An effort is made to quantify relevant experimental details, such as the increment of cutting depth. Sometimes the values reported here are given explicitly in the paper; other times they are estimated from graphs and figures.

The vast majority of the applications are to monolithic metals. Exceptions are Fett’s [19,20,21] applications to PMMA (Plexiglas) and PVC (polyvinyl chloride), Hermann’s [27] application to metal matrix composites, and a few applications to clad layers [22,24,39].

Table 1. Experimental Applications of the Crack Compliance Method, Chronological (key on next page)

	Solution		Slotting: a = depth, t = thickness (mm)				Component		Specimen	
Authors	**frwd**	**inv.**	**tool**	**a_f**	**da**	**a/t**	**measured**	**calc.**	**material**	**configuration**
Vaidyanathan & Finnie [52]	K_I	CF	saw	50	?	NA	K_I	σ_y	Al	butt-welded plates
Cheng & Finnie [2]	K_I	SE-L	MC	2	0.25	0.6	ε_θ-BF	σ_{ax}	304 stainless steel	circ.-welded thin cylinder
Cheng & Finnie [3]	K_I	SE-L	MC	42	1.6	~1	ε_θ-S	σ_θ	Al, 7050	quenched thin cylinder
Cheng & Finnie [4]	K_I	SE-L	MC	23	0.8-1.6	0.8	ε_θ-BF	σ_{ax}	304 stainless steel	butt-welded thin cylinders
Fett [19,20]	K_I-wf	SE-P	saw	33	0.6-3.0	0.65	COD-E	σ_y	PMMA	single-edge notched strip
Joerms [28]	NA	FEM	saw	?	?	0.5	COD-S,E	σ_θ	steel	railroad wheel
Ritchie & Leggatt [44]	FEM	IS-Q	MC	25	1.66	~1	ε_y -S,E,BF	σ_y,σ_{ax}	steel	bent beam, section of welded cylinder
Reid [42,43]	NA	CF	WEDM	28	0.25-0.5	~1	ε_y –BF	σ_y	steel	compact tension (CT) specimen
Kang et al. [29]	K_I-wf	IS	saw	80	2.0	0.6	COD, ε_y -S	σ_y	steel	butt-welded plates
Read [41]	NA	J	MC	14	1.0	0.28	ε_y -S,BF	J	steel	welded plate
Beghini & Bertini [1]	FEM	IS-Q	saw	75	1.0	~1	ε_y –E	σ_y	steel	welded plates
Cheng & Finnie [9]	K_I	SE-L	?	25	?	~1	ε_θ-S	σ_θ	4335V steel	quenched thick cylinder
Cheng et al. [12]	K_I	SE-L	WEDM	19	?	~1	ε_y –BF	σ_y	304 stainless steel	4-point bent beam
Gremaud+ [24], Cheng+ [16]	BF	SE-?	WEDM	1.0	0.025	0.05	ε_y –S	σ_y	stellite, steel	laser clad layer
Lai et al. [31,32]	K_I-wf	?	saw	14	NA	2	COD-E	σ_y	steel	ballised hole in plate
Cheng & Finnie [14]	K_I+FEM	SE-L	WEDM	159	1.3-5.1	0.96	ε_y -S,BF	σ_y	low carbon steel	in thick plate near attached bracket
Cheng et al. [15]	BF	SE-P	WEDM	0.8	0.025-0.05	0.05	ε_y –S	σ_y	304 stainless steel	4-point bent beam
Cheng et al. [16]	BF	SE-S	WEDM	0.65	0.013-0.025	0.02	ε_y –S	σ_y	Ti-6Al-4V	shot peened
Hermann [26]	NA	CF	WEDM	12	?	~1	ε_y –BF	σ_y	7017T651 Al	compact tension
Schindler et al. [45,46,49]	K_I	SE,IS	WEDM	140	1.3-15	~1	ε_θ-BF	σ_θ	tool steel	quenched solid cylinder
Perl & Aroné [37]	FEM	CF	saw	39.3	1.7-5.6	0.7	ε_θ-S,BF	σ_θ+	steel	autofrettaged thick cylinder
Hermann [27]	NA	CF	WEDM	12	?	~1	ε_y –BF	σ_y	Al-Li + SiC	compact tension MMC
Fett and Thun [21]	K_I-wf	SE-P	saw	90	5.0	0.9	COD-E	σ_θ	PVC	solid disks
Kang & Seol [30]	K_I-wf	IS	saw	18.6	0.8	~1	ε_θ-S	σ_θ	steel	water-quenched thick ring
Finnie et al. [22]	FEM	SE-L	WEDM	52	1.0	~1	ε_y -BF	σ_y	stellite, steel	laser-clad layer
Schindler & Landolt [47]	K_I-wf	IS	WEDM	12,30	continuous	~1	ε_y -S,BF	K_I ,σ_y	steel	bent beams
Galatolo & Laciotti [23]	?	?	MC	70	?	?	ε	σ_y	Al 2219	arc-welded plates
Nowell et al. [34]	DD	SE-F	WEDM	?	?	?	ε_y -?	σ_y	?	bent beam
Prime & Hellwig [39]	BF	SE-P	WEDM	3.8	0.13-0.25	0.18	ε_y -S,BF	σ_y	Cu on Al	laser clad
Schindler & Bertschinger [50]	K_I-wf	IS	WEDM	12	continuous	~1	ε_y –BF	K_I ,σ_y	high strength steel	bent beam
Schindler & Finnie [48]	K_I-wf	IS	WEDM	10,40	continuous	~1	ε_y –BF	K_I ,σ_y	mild steel	Charpy specimen, pre-cracked plate
Schindler [51]	K_I-wf	IS	WEDM	23,12	continuous	~1	ε_y –BF	K_I ,σ_y	stainless steel	2 CT & 1 beam specimens
Cheng & Finnie [18]	?	SE-L	WEDM	50	?	~1	ε_y –BF	σ_θ	Al 2024	water quenched rod & disk
Lim et al. [33]	K_I-wf	IS	saw	20	1.0	0.5	COD-E	σ_y	6061-T6 Al	ballised & indented hole in plate

Table 1 chronologically lists all of the experimental applications of the crack compliance method reviewed in this article. For each application, the table gives the theoretical approach, the details of making the slot, the deformation measurement and calculated stress component, and the material and geometry tested. A key to the abbreviations is given after the table. The reader is encouraged to consult the table for details not available in the text of this review.

Table 1. - Key

All Categories	**Cutting Tool**
NA not applicable	saw straight edge saw
? unspecified	MC milling cutter
	WEDM wire electric discharge machine
Forward Solution	**Measured Deformation Component**
K_I mode I stress intensity factor solution	ε_y, ε_{ax}, ε_θ normal, axial, hoop strain
K_I –wf using Bueckner's weight function	COD crack opening displacement
FEM finite element method	-S top surface (see Figure 1)
BF body force method	-BF back face "
DD dislocation density	-E edge "
Inverse Solution	**Calculated Stress Component**
CF closed form	σ_y, σ_{ax}, σ_θ normal, axial, hoop stress
SE series expansion	J J-integral
-L Legendre polynomials	K_I mode I stress intensity factor
-P power series	
-S splined (piecewise)	**Material/Specimen**
-F Fourier	PMMA Plexiglas
IS Incremental Stress	PVC polyvinyl chloride
-Q + least squares fit	MMC metal matrix composite
J J-Integral	CT compact tension

4.1 Rectangular Coordinates

This section reviews applications where residual stresses are measured in rectangular, or (*x*,*y*,*z*), coordinates. It is further divided into measurements of through-thickness or near-surface stresses.

4.1.1 Through-Thickness Stresses

This section reviews crack compliance method applications for measurement of residual stresses through the complete, or a substantial portion, of the part thickness. This approach is distinguished from near-surface stress measurements in that the effect of the back face free surface must be considered in the analysis, i.e., the forward solution. Strain measurements are often made on the back face instead of, or in addition to, on the top face near the slot. Since through-thickness residual stresses must satisfy force and moment equilibrium, this can serve as a constraint in the solution process or a check on the validity of results.

Fett [19,20] measured residual stress through about 65% of the thickness of a PMMA beam. A 50 mm thick beam was heated on one face to 120º C and held at room temperature on the opposite face and then quenched. Two indentations were made on one edge of the beam to allow COD measurements to be made with a microscope to a precision of about ±2 μm. A hand saw was used to cut the slot. The COD readings were taken 20 to 30 minutes after completing the cut, to allow cooling to equilibrium. A similar test on a stress-free specimen indicated that the sawing induced negligible stresses and would not affect the results. The residual stresses were calculated using a K_I forward solution and a power series expansion inverse. The results indicated that a 3rd order power series did not adequately describe the stresses or accurately reproduce the measured strains. The 4th and 5th order expansions were similar to each other and accurately reproduced the measured strains, indicating convergence in the expansion.

Ritchie and Leggatt [44] measured residual stress through the thickness of a cold bent beam. The 25 mm thick beam was made of BS 4360 Grade 50D structural steel. The beams were carefully stress relieved before bending in a four point fixture. A 2.4 mm thick saw was used to cut a slot in 1.66 mm increments through the beam thickness. Multiple gauges measured strains on the top surface, edge, and back face. A FEM solution, including the finite width of the slot, was the forward solution. The inverse solution was incremental stress combined with a least squares fit for the multiple strain readings. The results agreed well with a prediction for the residual stress profile based on an elastic perfectly plastic material. The results from using only back face strain data agreed well with those using all the strain gauges. Tests using the same procedure on a stress-relieved part indicated that errors from cutting induced stresses would not exceed ±20 MPa.

Reid [42] measured residual stress through the remaining ligament of a steel compact tension specimen. A standard geometry 25 mm thick compact tension specimen of mild steel was compressively preloaded to produce residual stresses. Reid was the first crack compliance method researcher to machine the slot using wire electric discharge machining (wire EDM). A 0.25 mm diameter wire made the cut in 0.25 to 0.5 mm increments from the tip of the machined notch to the back face, where a gauge measured the released strains. Reid's closed form inverse was used to solve for the stresses as a function of depth. To perform the inverse, the measured strains as a function of slot depth were fit with two 6th order splined polynomials. Reid noted that the calculated stresses satisfied equilibrium in the cross section to within 5%. Reid et al. [43] compared the results in this specimen with neutron diffraction results and used the results to predict crack growth rates in a fatigue test.

Kang et al. [29] measured residual stresses across a butt-welded plate. Two 10 mm thick steel plates were butt-welded together using gas metal arc welding. Each plate was 50 mm long in the direction normal to the weld line. A crack was introduced from one edge of the plate in 2 mm increments using a 0.6 mm thick hand saw. A second saw with a sharp tip was used before each strain measurement to best approximate a mathematical crack. At 50 mm depth, the slot passed through the weld line, and it was continued an additional 30 mm. Two top surface gauges, located 50 mm on either side of the slot, measured strains. An extensometer also measured COD. The authors used a weight function K_I solution as the forward solution. The

inverse solution was incremental stress using 6 mm increments, three times the cutting increment. The strain measurements on either side of the slot were averaged and then smoothed before inversion. The results using strains and those using COD agreed fairly well. The results were compared with hole drilling measurements.

Read [41] measured the *J*-integral due to residual stress near a weld in a steel plate. To prepare specimens, a 5 cm thick A-387 Grade 22 steel plate was cut with troughs 5 cm wide, 3.2 cm deep, and 20 cm long. The troughs were filled by welding. The slot was cut perpendicular to the weld using a 7.5 cm diameter circular saw. This resulted in a crack with a circular front and with a length that varied as the depth increased. The slot was cut in 1 mm depth increments to a final depth of 14 mm. Readings from multiple strain gauges were used to calculate the *J*-integral. He estimated the uncertainty to be about ±20%.

Beghini and Bertini [1] measured residual stress fields in steel plates with various weld geometries. A laser created welds in the long direction of ferritic steel plates 20 mm thick, 500 mm long, and about 72 mm wide. A saw was used to introduce a slot in 1 mm increments from one edge. After reaching half-width, about 36 mm, cutting was started from the other edge and continued until the two slots met and the part separated. Five gauges measured strain on the plate face along the length of the cut. An enhanced incremental stress inverse, supplemented by a least squares fit and constraints to ensure force and moment equilibrium, gave linear stress variation in each increment.

Cheng et al. [12] measured residual stresses through the thickness of a beam having a known residual stress distribution. The beam was made of stress-relieved 304 stainless steel, had a 19 mm square cross section, and was cold bent in a four-point bend fixture. Strains measured on the top and bottom surfaces during bending allowed the computation of the residual stress distribution from stress-strain curves measured during the actual bending. A slot was introduced using wire EDM, and strain was measured with a gauge on the back face directly opposite the cut. The authors used a K_I forward solution [10] and a Legendre series expansion inverse. They found close agreement between expansions with orders 7, 8, and 9. The results agreed very closely with the known distribution, in spite of the low magnitude of the residual stress distribution, which was less than 100 MPa throughout.

Cheng and Finnie [14] measured stress through the thickness of a plate at the toe of a welded attachment. A 50.8 mm wide bracket was welded to a 166 mm thick A533-B low carbon steel plate. Wire EDM was used to machine a 0.33 mm wide cut through the 166 mm thickness. Three gauges on the back face measured the released strain. The K_I forward solution for an edge notched strip [10] was combined with a numerical procedure to include the effect of the attachment. The inverse solution was a Legendre series expansion with the uniform and linear terms set to zero to ensure force and moment equilibrium. They averaged the 8th and 9th order expansion results to reduce the endpoint instability that is characteristic of polynomial expansions. Cheng and Finnie [9] briefly reported other results on a similar specimen.

Hermann [26] measured residual stress in the uncracked ligament of an aluminum compact tension specimen. Ten mm thick 7017-T651 aluminum compact tension specimens were compressively preloaded to three different load levels. A slot was incrementally extended using wire EDM from the tip of the pre-existing notch to the back face, about 12 mm. The measured strains as a function of depth were fit with a 5th order polynomial and then inverted to residual stresses using the approximate closed form inverse of Reid [42]. The results clearly demonstrated the effect of the preload magnitude. Hermann [27] repeated these test on specimens of 8090 Al-Li reinforced with 17 vol% silicon carbide (SiC). The study again compared various preloads and also looked at specimens without the SiC reinforcement.

Finnie et al. [22] measured residual stress through the thickness of laser-clad parts. Stellite F was clad to a 40 mm thick substrate of 304 stainless steel. The final layer thicknesses varied from 12 to 20 mm for different specimens. In some tests the substrate was preheated in an attempt to reduce tensile residual stresses. Wire EDM incrementally introduced a slot in 1 mm increments starting from the clad surface, using a 0.25 mm diameter wire. In the first test on a specimen prepared without preheating the substrate, a crack spontaneously propagated during machining of the slot. In subsequent tests on the non-preheated specimens, the strain gauge was placed on the clad surface and the slot started from the other face. The FEM forward solution accounted for the layer and substrate having different widths in the out-of-plane (z) direction. For the preheated specimens, a strength of materials correction accounted for out-of-plane bending caused by high compressive stresses. They used a series inverse with Legendre polynomials and separate series in the layer and substrate. Their results agreed well with a computer simulation.

Schindler and Landolt [47] measured both K_I and residual stresses in two different bent steel beams. In both cases wire EDM was used to make a slot about 0.3 mm wide. On one beam the strains were only measured on the back face, and on the other strains were measured on the top surface as well. The K_I from residual stresses was calculated directly from the strains and then used to determine residual stresses using an incremental stress inverse [46].

Schindler and Finnie [48] measured both K_I and residual stresses in pre-cracked steel plates. They examined a Charpy specimen with a 2.5 mm long fatigue pre-crack (a/t = 0.25) and a plate with a 20 mm long pre-crack (a/t = 0.5). K_I was calculated directly using strains measured at the back face [46,49]. Then an incremental stress inverse gave residual stresses from the K_I values. In one of the specimens, the residual stresses were high enough to cause yielding during the slot cutting and a correction was made for this nonlinearity.

Nowell et al. [34] measured residual stress through the thickness of a bent beam. Their purpose was to demonstrate the applicability of dislocation density analysis to the forward problem. Results from a 5 term Fourier series expansion inverse agreed well with predictions.

Schindler [51] measured crack closure stresses as well as residual stresses in several specimens. He argued that contact stresses in the closure zone of a fatigue crack could be considered a special type of residual stresses and measured in the same manner. He fatigued two compact tension specimens of austenitic stainless steel such that each had a fatigue crack about 3 mm long. One of the specimens was subsequently overloaded to remove crack closure effects. The slot was introduced using wire EDM, and K_I and the residual stress were calculated using Schindler's inversion technique [46,49]. The results clearly demonstrated the ability to measure the crack closure stresses. Closure stresses were also measured in a beam specimen with a 0.5 mm fatigue crack.

4.1.2 Near-Surface Stresses

This section reviews crack compliance method applications for measurement of stresses near the surface, defined by the slot penetrating a small enough fraction of the full thickness that the part can be considered semi-infinite for analysis purposes. For such measurements, strain or displacements must be measured on the free surface and close to the slot. The strain readings measured close to the slot will saturate at some depth and no longer be useful for determining stresses, see Section 3.2.1. It may be important to make a narrow slot and control its depth precisely. The width of the slot should be considered when the slot depth is less than five times the width, see Section 3.3. Because of the proximity of the gauge to the machined slot, stresses introduced during cutting can affect the results.

Several applications that were reviewed in the through-thickness section also included surface stress measurements. Ritchie and Leggatt [44] measured strains on the top face near the cut, in addition to the edge and back face, to improve the near-surface portion of their through-thickness measurements. They also used an FEM solution that included the finite width of the slot. Cheng and Finnie [14] and Schindler and Landolt [47] also supplemented back face strain measurements with strains measured on the top face near the cut to improve the surface stress portion of their measurements.

Gremaud et al. [24] measured stresses through the thickness of a laser-clad layer and into its substrate. A 0.58 mm layer of Stellite 6 was clad to a carbon steel substrate using a fast axial flow CO_2 laser. Careful mechanical grinding and subsequent sanding prepared the surface for strain gauging. The slot was introduced in 25 μm increments using wire EDM and a 51 μm diameter molybdenum wire. The authors used a body force method forward solution for edge notches of finite width [13]. Because the elastic constants for steel and Stellite are close, a solution for a single material was acceptable. The inverse solution was a series expansion, apparently using separate series in the layer and substrate. The results are qualitatively compared with x-ray results and agree well except in one regard. The crack compliance method measured a small region of compressive stress in the substrate steel just below the interface that was not measured by x-rays. Subsequent metallographic analysis revealed a martensitic transformation in this region. Such a phase change is accompanied by a volume expansion that generally produces compressive residual stress. This result gives strong evidence of the crack compliance method's ability to resolve variation with depth. Cheng et al. [16] revisited this test and reduced the same data using a piecewise series expansion to improve the results.

Cheng et al. [15] measured stresses in a specimen that had an accurately known residual stress distribution in order to evaluate the application of wire EDM to crack compliance measurements. A beam of 304 stainless steel was bent in a four-point fixture. A slot was introduced using a 51 μm diameter molybdenum wire. One cut was made on the tensile stress side of the beam with the EDM machine in "finishing mode," which involves more gentle, but slower, machining. The stress distribution agreed quite well with the known one and agreed almost exactly when the slight EDM correction was applied. A second cut was made on the compressive stress side with the EDM machine in "roughing mode." The results agreed with the known distribution after the EDM correction. With the roughing mode cut, the correction was fairly substantial, but this was considered to be partially because of the low magnitude of the residual stresses. Cheng et al. [12] and Gremaud et al. [24] reported results from very similar tests on specimens prepared in this same manner.

Cheng et al. [16] measured the near-surface residual stress distribution on a shot-peened titanium part. The specimens were 43 mm thick and made of Ti-6Al-4V. The slot was made using EDM with a 25 μm wire to a final depth of 0.65 mm. A small surface gauge, placed as close as possible to the cut, measured the released strains. Tests on a stress-relieved specimen indicated that the cutting had no effect on the strain measurements. The body force method forward solution included the finite width of the cut [13]. The inverse solution was a piecewise series expansion, with three quadratic functions over the first 14 data points and linear functions over the next 5 intervals. Results were presented for two tests on the same specimen and agreed well. The compressive peening stresses existed in only the first 100 μm of depth and appeared to be well resolved by this method. The results compared favorably with x-ray results.

Prime and Hellwig [39] measured residual stress in a laser-clad layer and into the underlying substrate. A 1 mm thick layer of a copper alloy (E = 124 GPa) was laser clad to a 20 mm thick substrate of aluminum (E = 72 GPa). A slot was cut using wire EDM and a 0.25 mm diameter wire to a final depth of 3.8 mm. The body force method forward solution included the finite width of the slot and in the difference in the elastic constants [38]. The series

expansion inverse solution used a single cubic expansion in the layer and overlapping piecewise power series [25] in the substrate. The results were compared to x-ray measurements.

4.1.3 Interior Stresses

This section reviews the infrequent crack compliance method applications for measuring residual stresses interior to a plate or other structure. In these cases, the slot is not started from an exterior free surface. Instead, it is started by drilling a hole in the interior or by using a pre-existing hole. The forward solution usually considers the free surfaces (other than the hole) to be at infinity and not to affect the stresses relieved by making the slot. For such a geometry, the deformations must be measured on the edge rather than on a face, by our definitions in Figure 1.

Vaidyanathan and Finnie [52] measured residual stresses in the interior of a plate made by butt welding two aluminum plates together. The plates, 6.35 mm thick 6061-T6 aluminum, were joined using electron beam welding. Using the coordinates of Figure 4, one plate would be defined by $x > 0$ and the other by $x < 0$, with the weld line running along the y-axis. A 1.6 mm diameter hole was drilled 50 mm in the x-direction from the weld centerline. A slot was then extended from the hole in the x-direction towards the weld using a 0.15 mm thick "jeweler's saw," a hand saw. The slot was extended to and through the weld. K_I was measured at the slot tip at each increment using a photoelastic coating. The authors used a K_I forward solution and a closed form inverse to get $\sigma_y(x)$.

Several investigators have examined residual stresses near ballised, or cold-expanded, holes in plates. In this process, a ball or other object is forced through a slightly smaller hole, producing compressive residual stress and an improved surface finish. Lai et al. [31] ballised 10 mm thick plates of medium carbon steel using a 19 mm diameter tungsten carbide ball. Axial saw cuts were introduced at opposite edges of the hole in 2 mm increments to lengths of 14 mm each. Displacements were measured using two points separated by 60 mm on opposite sides of the hole and on a line perpendicular to the slot. A traveling microscope measured the displacements to ±0.5 μm precision. The inverse solution was not specified but appeared to be an incremental stress procedure. The results showed the compressive stresses near the hole changing to balancing tensile stresses farther away. Oh et al. [35] discussed these results further and compared them to a theoretical prediction. Lai and Siew [32] repeated these tests with different specimens in which the hole was finished by ballising, wet blasting, and shot peening. They correlated the residual stress results with fatigue life. Lim et al. [33] performed similar measurements on 6 mm diameter holes in 2 mm thick aluminum plates. Some holes had the residual stress distribution changed by a ring-indentation technique applied after ballising. The residual stress measurements were correlated with fatigue crack growth rates.

Fett and Thun [21] measured hoop stress in a solid PVC (polyvinyl chloride), cylinder. In some of the tests, the slot was extended from the center of the disk and the COD was measured at the center. Unlike the other applications in this section, the free surface (outer radius) effects were included in the analysis. This work is further discussed in 4.2.2.

Galatolo and Lanciotti [23] measured residual stress in welded plates. Plasma arc welding made a weld along the centerline of 7 mm thick aluminum 2219-T851 plates. Few of the testing details are given. A central cut was extended progressively so as to simulate the growth of a crack across the weld bead. Measured strains were used to calculate residual stresses as a function of the crack length. The method of solving for stresses was not stated.

4.2 Cylindrical Coordinates

This section reviews measurements of axial and hoop, also known as circumferential, residual stresses in cylindrical coordinates.

No experimental applications of directly measuring radial stress with the crack compliance method are available, because of the difficulty of releasing the stress component by a slot. However, there are ways to determine radial stress from other measurements *if* the stresses are axisymmetric; as has been noted by several researchers [18,45,56]. The radial equilibrium equation reduces to

$$\frac{d\sigma_r}{dr} + \frac{\sigma_r - \sigma_\theta}{r} = 0 \ , \qquad (9)$$

which, combined with $\sigma_r = 0$ at the free surface, gives one the radial stress profile from the hoop stress profile. This is rarely applied because the radial stresses are small and rarely contribute to failures, so they are generally of little interest.

4.2.1 Axial Stress

In this section, crack compliance method applications for measuring residual axial stress in cylindrical geometries are considered. This involves introducing a circumferential slot in order to release the stresses. The slot may proceed from the outside surface in, or vice versa. Either released hoop or axial deformations may be measured on the cutting surface or the back face. Some investigators measured stresses in a thin ring cut from a long cylinder. All of the applications which involve cutting a circumferential slot assume that the stresses are axisymmetric.

A circumferential slot is more difficult to produce than an axial slot, which may account for the limited application of this technique for axial stresses. Cheng et al. [56] present a method to deduce plane-strain axial residual stresses from hoop stresses measured in a long cylinder and in a thin ring cut from the cylinder. This approach was applied by Cheng and Finnie [18] and is reviewed in 4.2.2.

Cheng and Finnie [2] measured axisymmetric axial residual stresses in a circumferentially welded thin-walled cylinder. The cylinder was 3.3 mm thick, 66 mm in diameter, and made of 304 stainless steel. An electron beam made a single-pass weld around the circumference of

the cylinder in the middle of the cylinder's 71 mm length. The heating conditions were such that the weld penetrated to the inner wall. A circumferential slot was made using a 0.23 mm thick milling cutter. The cut started at the inner surface and progressed in 0.25 mm depth increments toward the outer surface until the cutter broke about 62% of the way through the thickness. Three strips of 10 strain gauges each were mounted on the outer surface of the cylinder, separated by 120º around the circumference. On each strip the gauges measured hoop strain with the first gauge on the weld centerline and each successive gauge 2 mm further away from the weld. The data reduction used the average of the three gauges at the same distance from the weld. A K_I forward solution and a Legendre series expansion inverse up to order 3 were used to get $\sigma_{axial}(r)$. An analytical prediction of the welding residual stresses agreed well with the measurements.

Cheng and Finnie [4] measured axisymmetric axial residual stresses in a multi-pass circumferentially welded cylinder. The specimen tested was two cylinders of 304 stainless steel butt welded together using 22 weld passes. The cylinders were 16.5 mm thick with a mean diameter of 307 mm. At each of four locations around the cylinder circumference, three strain gauges oriented to measure hoop strain were placed 57 mm to 70 mm axially away from the weld centerline. These distances were chosen so as to locate the gauges in the region where the strain measurements were expected to vary minimally with distance from the weld. A circumferential cut was made from the inner wall along the weld centerline using a 0.8 mm thick milling cutter. The stresses were calculated using the average strain readings of the three gauges at each location, fit with a sixth order polynomial. A K_I forward solution and a series expansion inverse were used to solve for the stresses. The expansion used a fourth order Legendre series, excluding the 0th order term to ensure force equilibrium. The results obtained at the four circumferential locations agreed fairly well and agreed qualitatively with other available data.

Ritchie and Leggatt [44] measured residual axial stresses in a section cut from butt-welded cylinders. Two 25.4 mm thick steel cylinders with 761 mm outer diameters were butt-welded together using submerged arc welding. To avoid having to circumferentially slot such a large cylinder, strips including the weld sections were removed for subsequent slotting. Twenty strain gauges were placed on each section before removal to allow calculation of stress changes from removing the section. A slot was introduced in 1.66 mm increments using a 2.4 mm wide milling cutter through the weld. The back face and an edge were outfitted with 5 strain gauges each to measure released strains. A FEM solution including the finite width of the slot was the forward solution. The inverse solution was incremental stress combined with a least squares fit for the multiple strain readings.

4.2.2 Hoop Stress

In this section, crack compliance method applications for measuring residual hoop stress in cylindrical geometries are considered. Unlike axial stress measurements, no axisymmetry assumption is inherent in the measurements. However, some researchers use equilibrium constraints which apply only to axisymmetric stresses.

Cheng and Finnie [3] measured axisymmetric residual hoop stresses through the thickness of a quenched thin cylinder. They used two water-quenched 7050 aluminum cylinders 42 mm thick with mean diameters of 378 mm. An axial cut was made using a 0.8 mm wide milling cutter, starting at the outer surface and progressing completely through the thickness. Gauges measured hoop strains at 15º, 30º, 90º, and 120º circumferentially from the cut on the outer surface. The measured strains were fit with a 6th order polynomial before solving for stresses. A K_I forward solution and 4th order Legendre series expansion inverse were used to get $\sigma_\theta(r)$.

Joerms [28] measured residual hoop stresses in a steel railroad car wheel. The wheel geometry varied in the out-of-plane (z) direction, unlike most of the situations considered in this article. An axial saw cut was made radially inward from the outer surface of the wheel about half way to the center. COD was measured at the outer surface and along the full length of the cut at each increment. These measurements were used to generate a displacement map on the entire surface of the cut. These displacements were applied to a finite element mesh of the railroad wheel, to model forcing it back to its undeformed geometry. Joerms considered the resulting stress distribution to be a possible, though not necessarily unique, solution for the original residual stresses.

Cheng and Finnie [9] measured residual hoop stress through the thickness of a quenched, thick-walled cylinder. A 2.5 cm thick, 8.45 cm outer diameter 4335V steel cylinder was quenched in water from a temperature of 1160º K. The Legendre polynomial series inverse set the 0th order term to zero to ensure equilibrium. A fifth order series was found to sufficiently represent the stress field. The results were compared with a FEM calculation and x-ray surface measurements, and agreed very well with both.

Perl and Aroné [37] measured autofrettage levels (see 3.1.2) in a thick-walled cylinder. The cylinder was a steel gun barrel, with inner radius 52.5 mm and outer radius 113.0 mm. Seven cuts, equally spaced along the circumference, were extended from the inner surface to the outer surface using a band saw. Gauges measured hoop strain on the inner surface between cuts. They were able to calculate the autofrettage level from the measured strain.

Schindler et al. [45,46] measured residual hoop stress through the thickness of a large solid cylinder. The quenched and tempered tool steel cylinder was 140 mm in diameter, and stresses were measured in a disk 6.4 mm wide that was cut from the center of a long piece. Cuts were made radially inward using wire EDM. In Schindler et al. [45] the K_I forward solution interpolated between exact solutions for very shallow and very deep cuts. The

Legendre polynomial series expansion inverse set the first two terms to zero to ensure equilibrium. The solution was found to converge for a 4th order series. The results compared favorably with results from other crack compliance measurements made after drilling a hole in the disk. In Schindler [46] the same data was used with a different K_I weight function solution. The results from an incremental stress inverse agreed well with the previous results.

Kang and Seol [30] measured residual hoop stress through the thickness of a water-quenched steel ring. The medium carbon steel ring was 4 mm thick and had an outer diameter of 62 mm and an inner diameter of 42 mm.[1] A saw made a cut from the outer surface radially through the thickness of the ring. Just before completion of the final cut, the slot faces closed at the outer surface. Gauges located 90 degrees circumferentially on both sides of the cut measured the hoop strains on the outer surface. The average of these two gauges was smoothed using a polynomial technique and then used in data reduction. The incremental stress inverse used 2.4 mm steps, three times the cut increment. The results compared favorably with results from a sectioning method.

Fett and Thun [21] measured residual hoop stress in a solid PVC cylinder. Several disks 5 to 10 mm thick were cut from a 100 mm diameter PVC cylinder. In some of the specimens, a saw introduced a 0.5 mm wide edge cut along a diameter starting from the outer radius. An optical method gave crack opening displacements near the outer surface. In other specimens an internal cut was extended symmetrically from the center of the disk, and the crack opening was measured at the center. Power series expansion inverses enforced symmetry about the disk center for the internal crack tests only. Results from the two types of tests agreed well. The edge crack tests appeared to provide better results for near-surface stresses, and the internally cracked tests worked better for deeper subsurface stresses.

Cheng and Finnie [18] used crack compliance measurements to verify the results of a new "single slice" technique they developed for axisymmetric plane-strain stresses. They water quenched a 5.0 cm diameter rod of 2024 aluminum. They measured residual hoop stress by cutting a diametrical slot using wire EDM in both the plane strain rod and a plane stress disk cut from the rod. The Legendre series inverse used only the even terms because of the symmetry. The plane stress and plane strain hoop stress results allowed them to analytically calculate the original plane strain axial residual stresses [56].

4.3 Cutting Methods

Several different techniques have been used to introduce the slots for the crack compliance method. Some are easier to implement than others, and some have effects on the measurements. This section briefly discusses the relevant issues for each.

Saws are commonly used to make the cuts. Here, saws are taken to mean a saw with a straight edge, as compared to circular-shaped saws. Such saws include band saws, jig saws, and hand saws. Saws as thin as 150 μm [52] have been used. When a slot is cut into a compressive stress field, the slot may close up and pinch the saw. Kang and Seol [30] had a slot close on itself when trying to cut through the thickness of a ring, but only when the remaining ligament was very small. Kang et al. [29] used a saw with a tapered profile, narrower at the back, to prevent pinching the saw. They also sharpened the slot tip to better approximate a crack (see 3.3 for a discussion of slot shape) using a second saw.

Milling cutters also are used to machine slots. A milling cutter uses a circular, rotating saw blade to cut the slot. Using the table adjustments on the mill can make alignment of the cut in subsequent passes and the cut depth more precise than for saws. Cutters as thin as 230 μm [2] and as thick as 2.4 mm [44] have been used. Thin cutters may break during cutting, and restarting the cut after a break is often impossible [2,4].

Mechanically machining the slot, using a saw or milling cutter, is likely to introduce residual stresses. Several investigators have measured the stresses induced by cutting on a stress-free specimen and found that the machining induced only small errors in measured residual stresses, for the proper cutting parameters [19,20,44]. Machining the slot can also cause local temperature increases. Fett [19,20], after making a saw cut, had to wait 20 to 30 minutes to take strain readings in order to let the temperature equilibrate in plastic specimens.

Wire EDM has become the method of choice for cutting the slot, see Table 1. Reid [42] was the first to use wire EDM to make the slot for crack compliance measurements, although its advantages for residual stress measurement have been recognized for some time [e.g., 58]. In wire EDM, the wire is electrically charged with respect to the workpiece. As the wire approaches the workpiece, a spark jumps the gap and locally melts and removes material. The wire advances as material is removed. The cutting occurs in a dielectric fluid, usually deionized water, and the wire never actually contacts the workpiece.

There are two main advantages to using EDM instead of conventional machining. First, a much finer slot may be cut. Cheng et al. [16] made the smallest known slots for crack compliance measurements, using a 25 μm diameter wire for two near-surface tests on a titanium alloy to make slots approximately 32 and 42 μm wide.[2] A 50 μm diameter is more commonly used for near-surface measurements [15,16,24]. For deeper or through-thickness measurements, researchers use wires from 100 μm [12,39] to as large as 250 μm diameter [22,39,42,47,50]. Second, EDM can cut much more gently than conventional machining and,

[1] These dimensions are given as radii, not diameters, in the paper, but they must be diameters to be consistent with other dimensions in the paper.

[2] Private communication, Weili Cheng, February 1997.

therefore, not introduce significant stresses. In fact, EDM quite easily cuts hard materials that can be very difficult to machine conventionally, such as martensitic steels. Another possible advantage of wire EDM is that one could make the cut continuously rather than incrementally. Schindler and co-workers [47,48,50,51] have done so, and they discuss it briefly [50]. It should also be noted that wire EDM can only be used on electrically conductive material. Additionally, it may be difficult to cut an EDM slot with a fine wire when the material has non-conducting phases or inclusions [39].

Although wire EDM generally introduces less stress than conventional machining, it can still affect measurements for very near-surface stresses when the strain gauge is very near the slot. Cheng et al. [15] thoroughly investigated the use of wire EDM for near-surface residual stress measurement. They mentioned that cutting conditions and material properties have a large effect on the possibility of introducing residual stresses during cutting. In general, larger thermal expansion and lower thermal conductivity will increase the stresses introduced. Also, cutting in "roughing" mode introduces more stress than cutting in "finishing" mode. Finishing mode refers to cutting parameters designed to provide an improved surface finish using an additional cut after an initial cut in roughing mode. These parameters can usually be obtained from the EDM machine manufacturer. Cheng et al. developed and experimentally verified a technique to correct for the stresses introduced by wire EDM cutting during residual stress measurements. They performed tests on a 304 stainless-steel beam in both roughing and finishing mode. Corrections were successful in both cases and minimal for the finishing mode test. In general, one should use the wire EDM machine settings for finishing cuts for crack compliance measurements whenever possible.

5 COMPARISONS WITH OTHER METHODS

This section qualitatively compares the crack compliance method to the most common residual stress measurement techniques: x-ray diffraction, neutron diffraction, hole drilling, and layer removal. For the purposes of this discussion, x-ray and neutron are grouped as diffraction methods, and crack compliance, layer removal, and hole drilling are grouped as mechanical methods. These methods are compared with regard to destructiveness, sensitivity, depth profiling, accuracy, measuring time, and stress components measured. Lu et al. [62] contains a more detailed comparison between measurement techniques, but the crack compliance method is not included.

These comparisons reveal that there is no single best method for measuring residual stress. The selection of a method should consider the particular application and the strengths and weaknesses of all methods.

5.1 Destructiveness

The only method considered here that can nondestructively measure residual stress variation with depth is neutron diffraction, but it has resolution and size limitations. Neutron diffraction can measure to depths of tens of millimeters but can only resolve stresses in regions approximately 1 mm^3 or larger. Additionally, because of penetration limitations, neutron diffraction generally cannot be applied to parts larger than about 50 mm thick. However, crack compliance had been applied to parts as thick as 166 mm [14].

The other methods are destructive to different degrees. X-ray diffraction can measure only very near-surface stresses nondestructively. Depth profiling requires etching away layers at the spot to be measured. Hole drilling and crack compliance are considered semi-destructive methods. They both require local material removal, with crack compliance generally more destructive. Layer removal is a destructive method in which layers are removed from the entire surface of a part. A complete residual stress profile by removing layers will destroy the part.

5.2 Sensitivity

Sensitivity refers to the level of data measurement for low residual stress levels. The mechanical methods measure strain caused by releasing residual stress, and the measured strains can be small for low stresses. Layer removal generally has the lowest sensitivity, but this sensitivity depends greatly on the part thickness. Hole drilling has increased sensitivity, and crack compliance has even greater sensitivity. Cheng et al. [8] explicitly compared the sensitivity of crack compliance to hole drilling and showed compliance to be significantly more sensitive. One possible drawback of sensitivity is that it generally also corresponds to a greater propensity to yielding at high stress levels, which leads to errors.

The diffraction methods also have difficulties measuring low stresses but for a different reason. They measure crystal lattice spacing. Because this spacing is only slightly changed by residual stress levels, diffraction methods can measure the spacing corresponding to low stresses as easily as high stresses. For example, 1 angstrom is about as easy to measure as 1.1 angstrom. However, the uncertainty in these measurements is approximately constant at $\pm 50\ \mu\varepsilon$ to $\pm 100\ \mu\varepsilon$ (see 5.4). So, for low residual stress (strain) levels, the uncertainty is proportionally higher.

5.3 Depth Profiling

Figure 6 shows the approximate depth ranges over which the various methods are able to resolve residual stress variations. The depth range shown for x-rays is for non-destructive measurements. Profiles up to 1 mm depth are commonly made with x-rays by electrochemically etching away material. The figure illustrates the need to consider two important factors when choosing a residual stress measurement method for a particular application: (1) the depth of residual stresses that was generated in

manufacturing the part of interest, and (2) the depth to which residual stresses will contribute to the potential failure mechanism.

Section 3.2.1 discusses spatial resolution for crack compliance in greater detail.

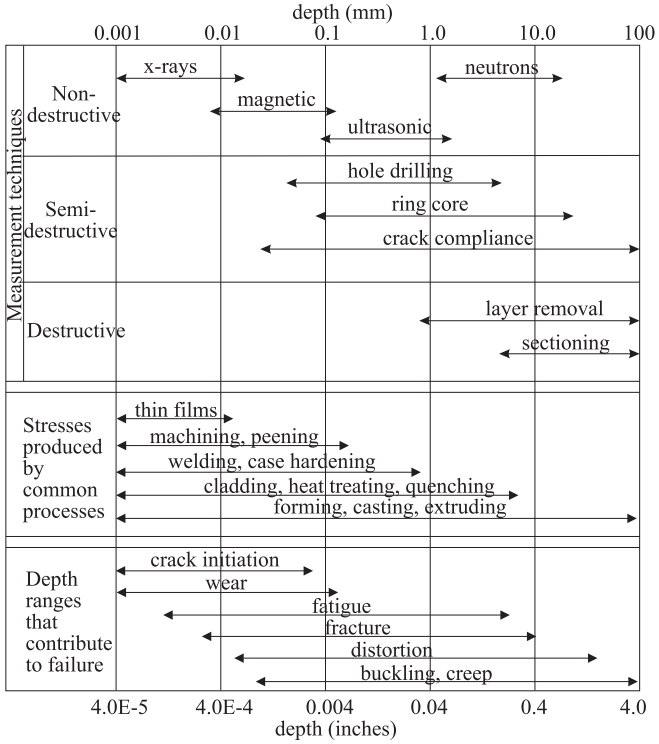

Figure 6. Depth ranges of measurement techniques compared with typically observed profiles and failure mechanisms. Similar to figure in Leggatt et al. [61].

5.4 Accuracy

A wide variety of factors influence the accuracy of all measurement methods. No single method can be considered the most accurate. Typically quoted values for the uncertainty of diffraction methods range from ± 50 με to ± 100 με, depending on the conditions. Similarly quoted values for mechanical methods are ± 10 MPa to ± 30 MPa, depending on the particular method and the conditions. For the elastic constants typical of engineering materials, these uncertainties are of similar magnitude. However, there are many situations that can determine where within these ranges, or even outside them, the results from a particular test could end up.

The x-ray and neutron diffraction methods are based on properties of the crystalline microstructure. The presence of multiple phases and texture (preferred orientation) can reduce accuracy in stress measurements. Because it measures a surface spot with little depth penetration, the x-ray method can give unexpected results because of the presence of a local surface effect, such as oxidation. Large grains can also increase errors using x-rays because the spot examined may contain too few grains to provide a sufficient statistical sample. The mechanical methods function virtually independently of microstructure.

The mechanical methods are susceptible to errors from several sources. Stresses induced during the material removal process will decrease the accuracy of the measurements. Also, if the stresses removed are excessively large, yielding can occur which increases errors because the calculations assume elasticity. There is another source of error for the hole drilling method. Because the analysis assumes a hole located in the center of the strain rosette, hole misalignment results in increased errors.

All of the methods, diffraction and mechanical, require elastic constants to calculate residual stress. Errors or uncertainties in the values of the elastic constants produce proportionally equivalent errors or uncertainties in the residual stresses. Calculation of residual stresses from x-ray or neutron measurements of single diffraction peaks requires plane-specific elastic constants, which are more difficult to find than bulk constants and may be less precise. Often, when plane-specific constants are not available, calculations are based only on an approximate relation to the bulk constants, which is another source of error.

5.5 Time Required for Measurements

The time to perform diffraction measurements depends on factors such as the material being examined and the sampling volume. Generally, neutron diffraction takes longer than x-ray, but x-ray requires extra time to etch away layers between measurements. Generating a profile typically takes one to several days for x-rays and several days or more for neutrons.

Experimental time for the mechanical methods is generally less than for diffraction methods. Layer removal takes the longest because it requires the most material removal. Crack compliance measurements can usually be taken in just a few hours. It should be noted that, prior to measurements, the mechanical methods typically require time to install strain gauges and for any protective coatings to dry.

For all of the methods, the total time to produce results depends on the complexity of the data reduction technique, with the most complex methods taking several days or longer.

5.6 Stress Components and Stress Versus Strain

To facilitate a discussion of the measured stress components, a review of the stress-strain relations is presented. In general, one needs to know all of the normal stress components to determine any of the normal strain components, and vice versa. For example:

$$\varepsilon_y = \frac{1}{E}\left[\sigma_y - \nu\left(\sigma_x + \sigma_z\right)\right], \qquad (10)$$

with similar equations for the x and z strains. E is the elastic modulus, and ν is Poisson's ratio. This set of equations can be solved for stresses in terms of strains to give

$$\sigma_y = \frac{E}{(1+\nu)(1-2\nu)}\left[(1-\nu)\varepsilon_y + \nu\left(\varepsilon_x + \varepsilon_z\right)\right] \qquad (11)$$

and similar equations for the x and z stresses.

The distinction between determining residual stresses or determining residual strains can be an important one. Since none of the methods determine all three stress or strain components in a single measurement, it is not always possible to convert strain measurements to stress or vice versa. For using results to predict or evaluate failures, such as fatigue, fracture, or distortion, one or more stress components generally must be known. For comparison with predictive models, either stress or strain is usually acceptable.

The diffraction methods determine residual strains. Neutron diffraction measurements from a spallation source (also known as time-of-flight or polychromatic) can measure two strain components in a single measurement, and neutron measurements using a reactor (monochromatic) will measure a single component. Multiple measurements may be able determine the whole strain tensor, but this is not always done. Measurements of just two strain components can only determine stress components if one makes some assumption about the state of stress, such as plane stress or plane strain. X-ray diffraction measures a difference between one of the in-plane strain components and the out-of-plane component, for example $\varepsilon_y - \varepsilon_x$ for measurements on the top face in Figure 1. Combined with the free surface condition, $\sigma_x = 0$, this is sufficient to determine σ_y from the elasticity relations of Eq. 10 or Eq. 11. A second measurement can give the other in-plane stress, σ_z.

The mechanical methods, although measuring a strain or displacement during the test, determine residual stresses. It is not possible to determine strain components from a subset of the stress components without making assumptions. However, strain measurements are rarely desired over stresses. Hole drilling and layer removal methods determine both stress components in the plane of the part, *y* and *z* components in Figure 1. Crack compliance measures the stress component normal to the slot, the *y* component in Figure 1. In many situations, only one stress component is of interest because only one affects the failure mechanism of concern.

Section 2.4 has a detailed discussion of measuring shear strains using crack compliance or hole drilling.

5.7 Miscellaneous

When cutting a slot into a high tensile residual stress field with crack compliance, a crack can possibly self propagate. Although uncommon, this has been reported [22]. Of course, a substantial amount of propagation would result in the end of the test and the destruction of the specimen.

Residual stresses can be divided into three types, depending on the length scales over which they act [62], and the measurement methods are not all influenced by the same types. Type I stresses, or continuum or macrostresses, vary over distances of at least several grains, and usually more. Type II stresses, or microstresses, vary on the length scale of grains. They occur commonly as variations between different phases or between inclusions and the matrix. Type III stresses vary over several atomic distances within the grain and are equilibrated over a small part of the grain. Mechanical methods are generally only affected by type I stresses. Diffraction methods are generally affected by the sum of type I and II stresses, although neutron measurements are taken over a sufficiently large volume to minimize the effects of type II stresses. The influence of type II stresses in a measurement can obscure the value of the type I stresses and hinder comparison with continuum scale predictions, such as finite element models. On the other hand, comparisons with polycrystal models are more appropriate with measurements of both type I and II stresses.

Accessibility is an important factor when choosing a method for measuring residual stress. Neutron sources are only available at a handful of institutions worldwide. However, many neutron facilities allow researchers to perform measurements at no cost. X-ray sources are much more common, although many are not ideally configured for residual stress measurements. Purchasing the equipment would cost on the order of $100,000. Several private companies will perform x-ray residual stress measurements for a fee. Hole drilling can be performed with standard equipment at a machine shop, but specialized equipment to improve accuracy costs on the order of $10,000. Again, some private firms will perform hole-drilling measurements for a fee. Crack compliance can be performed using equipment at a standard machine shop. Wire EDM machines, which cost on the order of $100,000, are standard equipment in many shops and can be used by paying an hourly fee. Layer removal measurements can be performed with standard machine shop equipment, or with a more specialized for electrochemical layer removal. Another possible issue is taking portable measurements, which can be made with specialized hole-drilling or x-ray equipment.

6 CONCLUDING REMARKS

The crack compliance method adds unique new capabilities to the current suite of residual stress measurement techniques. Compared to other destructive methods, crack compliance offers increased spatial resolution of residual stresses and increased sensitivity to low stresses. As seen in Figure 6, the sub-millimeter spatial resolution provided by crack compliance cannot currently be matched by the most common nondestructive techniques–x-ray and neutron diffraction. To achieve these gains, crack compliance sacrifices the ability of other techniques, such as the hole-drilling method, to measure all of the in-plane stresses. Other crack compliance advantages include a simple analytical technique to determine the stress intensity factor caused by a crack in a residual stress field and the ability to measure crack closure stresses. Furthermore, crack compliance can be applied fairly easily with commonly available equipment: strain gauges and electric discharge or conventional machining.

There is a need for further research to make the crack compliance method more generally applicable, accurate, and easier to apply. There is much room for improving the robustness of the current techniques for inverting from the measured strains back to the original residual stress. At the same time, the current techniques are computationally intensive and provide a barrier to more widespread application. Simpler techniques or some set of standard coefficients for an inversion scheme could help. This review also indicates that there is need for further research on identification of yielding during the measurement process and the implications for subsequently determining stresses.

Exciting opportunities exist for advances in the measurement of deformation during the slot cutting. Current crack compliance applications measure strain or displacement at a few discrete locations. Beyond this lies the possibility of measuring full field deformations at many locations or throughout an entire surface area, using interferometric or other techniques. Such measurements could result not only in improved spatial resolution, but also the determination of two-dimensional stress variations rather than just the current one-dimensional capability.

There are similarly exciting opportunities for advances made possible by new slot-cutting techniques. Novel slot shapes could be used to measure different stress components or to measure two-dimensional or even three-dimensional stress variation. Lasers could be used to cut arbitrary slot shapes, to cut in many materials that are otherwise difficult to cut, and to cut without introducing significant new stresses. Lasers or plunge EDM could be used to cut slots in the interior of large parts (not from edge to edge in the z-direction, see Figure 1).

The use of full-field deformation measures and novel slot shapes will require increasingly sophisticated techniques to invert from the measured deformations back to the original residual stresses. It will be a challenge to solve these problems without drastically increasing the computational complexity.

ACKNOWLEDGEMENTS

This work was supported by the Laboratory Directed Research and Development program at Los Alamos National Laboratory, which is operated by the University of California for the US Department of Energy under contact number W-7405-ENG-36. The author studied crack compliance with Iain Finnie and Weili Cheng at U.C. Berkeley and is grateful for the knowledge they shared. The author would also like to thank Carolyn Robinson for editing a previous version of this review.

7 REFERENCES

7.1 Crack Compliance Method References

1. Beghini M and Bertini L (1990), Residual Stress Modelling by Experimental Measurements and Finite Element Analysis, *J Strain Anal Eng Des*, **25**(2), 103-108.
2. Cheng W and Finnie I (1985), A Method for Measurement of Axisymmetric Residual Stresses in Circumferentially Welded Thin-Walled Cylinders, *J Eng Mat Tech*, **107**, 181-185.
3. Cheng W and Finnie I (1986), Measurement of Residual Hoop Stress in Cylinders Using the Compliance Method, *J Eng Mat Tech*, **108**, 87-92.
4. Cheng W and Finnie I (1987), A New Method of Measurement of Residual Axial Stresses Applied to a Multi-Pass Butt Welded Cylinder, *J Eng Mat Tech*, **109**, 337-342.
5. Cheng W and Finnie I (1988), K_I Solutions for an Edge Cracked Strip, *Eng Fracture Mech*, **31**, 201-207.
6. Cheng W and Finnie I (1990), A K_{II} Stress Intensity Solution for an Edge Cracked Strip, *Eng Fracture Mech*, **36**, 355-360.
7. Cheng W and Finnie I (1990), The Crack Compliance Method for Residual Stresses Measurement, *Welding in the World*, **28**, 103-110.
8. Cheng W, Finnie I, and Ö Vardar (1991), Measurement of Residual Stresses Near the Surface Using the Crack Compliance Method, *J Eng Mat Tech*, **113**, 199-204.
9. Cheng W and Finnie I (1991), An Experimental Method for Determining Residual Stresses in Welds, in *Modeling of Casting, Welding, and Advanced Solidification Processes - V*, Rappaz M (ed), The Minerals, Metals, and Materials Society, Warrendale, PA, USA, 245-252.
10. Cheng W, Finnie I, and Ö Vardar (1992), Deformation of an Edge Cracked Strip Subjected to Normal Surface Traction on the Crack Faces, *Eng Fracture Mech*, **42**, 97-107.
11. Cheng W and Finnie I (1992), Deformation of an Edge Cracked Strip Subjected to Arbitrary Shear Surface Traction on the Crack Faces, *Eng Fracture Mech*, **43**, 33-39.
12. Cheng W, Finnie I, and Prime MB (1992), Measurement of Residual Stresses Through the Thickness of a Strip Using the Crack Compliance Method, in *Residual Stresses III - Science and Tech, Proc Third Int Conf Residual Stress*, Vol. 2, Elsevier Applied Science, Fujiwara H, et al. (eds), 1127-1132.
13. Cheng W and Finnie I (1993), A Comparison of the Strains due to Edge Cracks and Cuts of Finite Width in a Semi-Infinite Elastic Plate, *J Eng Mat Tech*, **115**, 220-226.
14. Cheng W and Finnie I (1993), Measurement of Residual Stress Distributions Near the Toe of an Attachment Welded on a Plate Using the Crack Compliance Method, *Eng Fracture Mech*, **46**, 79-91.
15. Cheng W, Finnie I, Gremaud M, and Prime MB (1994), Measurement of Near Surface Residual Stresses Using Electrical Discharge Wire Machining, *J Eng Mat Tech*, **116**, 1-7.
16. Cheng W, Finnie I, Gremaud M, Rosselet A, and Streit RD (1994), The Compliance Method for Measurement of Near Surface Residual Stresses - Application and Validation for Surface Treatment by Laser and Shot-Peening, *J Eng Mat Tech*, **116**, 556-560.
17. Cheng W and Finnie I (1994), An Overview of the Crack Compliance Method for Residual Stress Measurement, *Proc Fourth Int Conf Residual Stress*, Baltimore, Maryland, Society for Exp Mechanics, 449-458.
18. Cheng W and Finnie I (1998), The Single Slice Method for Measurement of Axisymmetric Residual Stresses in Solid Rods or Hollow Cylinders in the Region of Plane Strain, *J Eng Mat Tech*, **120**, 170-176.
19. Fett T (1987), Bestimmung von Eigenspannungen mittels bruchmechanischer Beziehungen (Determination of Residual Stresses by Use of Fracture Mechanical Relations), *Materialprüfung*, **29**, 92-94.
20. Fett T (1996), Determination of Residual Stresses in Components Using the Fracture Mechanics Weight Function, *Eng Fracture Mech*, **55**(4), 571-576.
21. Fett T and Thun G (1996), Residual Stresses in PVC-Cylinders Determined with the Weight Function Method, *Eng Fracture Mech*, **55**(5), 859-863.
22. Finnie S, Cheng W, Finnie I, Drezet J-M, and Gremaud M (1996), The Computation and Measurement of Residual Stresses in Laser Deposited Layers, *Proc Fourth European Conference Residual Stress*, Cluny-en-Bourgogne, France, June 1996, Denis S et al. (eds), **1**, 183-192.
23. Galatolo R and Laciotti A (1997), Fatigue Crack Propogation in Residual Stress Fields of Welded Plates, *Int J Fatigue*, 19(1), 43-49.
24. Gremaud M, Cheng W, Prime M, and Finnie I (1992), Measurement of Residual Stresses in Laser Treated Layers Using the Crack Compliance Method, in *Proc Int Conf Laser Advanced Mat Proc*, Matasunawa A and Katayama S (eds), 713-718.
25. Gremaud M, Cheng W, Finnie I, and Prime MB (1994), The Compliance Method for Measurement of Near Surface Residual Stresses - Analytical Background, *J Eng Mat Tech*, **116**, 550-555.
26. Hermann R (1994), Fatigue Crack Growth in Ductile Materials Under Cyclic Compressive Loading, *Fatigue Fracture Eng Mat*, **17**(1), 93-103.
27. Hermann R (1995), Crack Growth and Residual Stress in Al-Li Metal Matrix Composites Under Far-Field Cyclic Compression, *J Mat Sci*, **30**, 3782-3790.
28. Joerms MW (1987), Calculation of Residual Stresses in Railroad Rails and Wheels from Sawcut Displacement, in *Residual Stress in Design, Process and Mat Selection, Proc ASM's Conf Residual Stress in Design, Process and Mat Selection*, Cincinnati, Ohio, USA, 27-29 April 1987, W. Young B (ed), 205-209.
29. Kang KJ, Song JH, and Earmme YY (1989), A Method for the Measurement of Residual Stresses Using a Fracture Mechanics Approach, *J Strain Anal Eng Des*, **24**, 23-30.

30. Kang KJ and Seol SY (1996), Measurement of Residual Stresses in a Circular Ring Using the Successive Cracking Method, *J Eng Mat Tech*, **118**, 217-223.
31. Lai MO, Oh JT, and Nee AYC (1993), Fatigue Properties of Holes with Residual Stresses, *Eng Fracture Mech*, **45**(5), 551-557.
32. Lai MO and Siew YH (1995), Fatigue Properties of Cold Worked Holes, *J Mat Processing Tech*, **48**, 533-540.
33. Lim WK, Yoo JS, and Choi SY (1998), The Effects of Concurrent Cold-Expansion and Ring-Indentation on the Growth of Fatigue Cracks Emanating from Circular Holes, *Eng Fracture Mech*, **59**(5), 643-653.
34. Nowell D, Tochilin S, and Hills DA (1997), The Crack Compliance Method for Measurement of Residual Stress: Dislocation Density Analysis, *The Fifth Int Conference on Residual Stresses*, Linköping, Sweden, June 1997, Ericsson T et al. (eds), **2**, 664-669.
35. Oh JT, Lai MO, and Nee AYC (1993), Stress Analysis of a Ballised Hole, *J Mat Processing Tech*, **37**, 137-147.
36. Orkisz J and Skrzat A (1996), Reconstruction of Residual Stresses in Railroad Vehicle Wheels Based on Enhanced Saw Cut Measurements, Formulation and Benchmark Tests, *Wear*, **191**, 188-198.
37. Perl M and Aroné R (1994), An Axisymmetric Stress Release Method for Measuring the Autofrettage Level in Thick-Walled - Parts I & II, *J Pressure Vessel Tech*, **116,** 384-395.
38. Prime MB and Finnie I (1996), Surface Strains Due to Face Loading of a Slot in a Layered Half-Space, *J Eng Mat Tech*, **118**, 410-418.
39. Prime MB and Hellwig Ch (1997), Residual Stresses in a Bi-Material Laser Clad Measured Using Compliance, *The Fifth Int Conference on Residual Stresses*, Linköping, Sweden, June 1997, Ericsson T et al. (eds), **1**, 127-132.
40. Prime MB (1999), Measuring Residual Stress and the Resulting Stress Intensity Factor in Compact Tension Specimens, to appear *Fatigue Fracture Eng Mat Struct*.
41. Read DT (1989), Measurement of Applied *J*-Integral Produced by Residual Stress, *Eng Fracture Mech*, **32**(1), 147-153.
42. Reid CN (1988), A Method of Mapping Residual Stress in a Compact Tension Specimen, *Scripta Metallurgica*, **22**(4), 451-456.
43. Reid CN, Moffatt J, and Hermann R (1988), Fatigue Under Compressive Loading and Residual Stress, *Scripta Metallurgica*, **22**, 1743-1748.
44. Ritchie D and Leggatt RH (1987), The Measurement of the Distribution of Residual Stress Through the Thickness of a Welded Joint, *Strain*, **23**(2), 61-70.
45. Schindler HJ, Cheng W, and Finnie I (1994), Measurement of the Residual Stress Distribution in a Disk or a Solid Cylinder Using the Crack Compliance Method, in *Proc Fourth Int Conf Residual Stress*, Baltimore, Maryland, Society for Exp Mechanics, 1266-1274.
46. Schindler HJ (1995), Determination of Residual Stress Distributions from Measured Stress Intensity Factors, *Int J Fract*, **74**(2), R23-R30.
47. Schindler HJ and Landolt R (1996), Experimental Determination of Residual Stresses and the Resulting Stress Intensity Factors in Rectangular Plates, *Proc Fourth European Conference Residual Stress*, Cluny-en-Bourgogne, France, June 1996, Denis S et al. (eds), **1**, 509-517.
48. Schindler HJ and Finnie I (1997), Determination of Residual Stresses and the Resulting Stress Intensity Factors in the Ligament of Pre-Cracked Plates, *Proc Ninth Int Conf Fracture*, Sydney, Australia, Karihaloo BL, et al. (eds), Pergammon Press, 523-530.
49. Schindler HJ, Cheng W, and Finnie I (1997), Experimental Determination of Stress Intensity Factors Due to Residual Stresses, *Exp Mech*, **37**(3), 272-277.
50. Schindler HJ and Bertschinger P (1997), Some Steps Towards Automation of the Crack Compliance Method to Measure Residual Stress Distributions, *The Fifth Int Conf on Residual Stresses*, Linköping, Sweden, June 1997, Ericsson T et al. (eds), **2**, 682-687.
51. Schindler HJ (1998), Experimental Determination of Crack Closure by the Cut Compliance Technique, to appear in *ASTM STP 1343, Advances in Fatigue Crack Closure Measurement and Analysis*, McClung RC and Newman JC Jr. (eds), American Society for Testing and Materials.
52. Vaidyanathan S and Finnie I (1971), Determination of Residual Stresses from Stress Intensity Factor Measurements, *J Basic Eng*, **93**, 242-246.

7.2 Other References

53. Abifarin MS and Adeyemi MB (1993), Residual Stresses in Squeeze-cast Aluminum Rods, *Exp Mech*, **33**(3), 174-180.
54. Archer RR (1987), *Growth Stresses and Strains in Trees*, Springer-Verlag, Berlin, Germany.
55. Bueckner HF (1958), The Propagation of Cracks and the Energy of Elastic Deformation, *Trans Amer Soc Mech Eng*, **80**, 1225-1230.
56. Cheng W, Finnie I, and Vardar Ö (1992), Estimation of Axisymmetric Residual Stresses in a Long Cylinder, *J Eng Mat Tech*, **114**, 137-140.
57. Clutton EQ and Williams JG (1995), On the Measurement of Residual Stress in Plastic Pipes, *Polymer Eng Sci*, **35**(17), 1381-1386.
58. Ellingson WA and Shack WJ (1979), Residual-Stress Measurements on Multi-Pass Weldments of Stainless-Steel Piping, *Exp Mech*, **19**(9), 317-323.
59. Fett T and Munz D (1997), *Stress Intensity Factors and Weight Functions.* Computational Mechanics Publications, Southampton, UK.
60. Kelsey RA (1956), Measuring Non-Uniform Residual Stresses by the Hole Drilling Method, in *Proc Soc Exp Stress Anal*, **14**(1), 181-194.
61. Leggatt RH, Smith DJ, Smith SD, and Faure F (1996), Development and Experimental Validation of the Deep Hole Method for Residual Stress Measurement, *J Strain Anal Eng Des*, **31**(3), 177-186.
62. Lu J, James M, and Roy G, Editors (1996), *Handbook of Measurement of Residual Stress*, The Fairmont Press, Inc., Lilburn, Georgia, USA.
63. Midha PS and Modlen GF (1976), Residual Stress Relief in Cold-Extruded Rod, *Metals Tech*, 529-533.
64. Nisitani H (1978), Solutions of Notch Problems by Body Force Method, in *Stress Analysis of Notch Problems*, Sih GC (ed), Vol. 5 of *Mechanics of Fracture*, Nordhoff International Publishing, 1-68.
65. Ovseenko AN (1981), Determination of the Axial Residual Stresses in Cylindrical Rods by the Longitudinal Incision Method, *Strength Mat*, **13**(7), 852-858.
66. Perl M (1998), An Improved Slit-Ring Method for Measuring the Level of Autofrettage in Thick-Walled Cylinders, *J Pressure Vessel Tech*, **120**, 69-73.
67. Petrucci G and Zuccarello B (1996), Effect of Plasticity on the Residual Stress Measurement Using the Groove Method, *Strain*, **32**, 97-103.
68. Petrucci G and Zuccarello B (1997), Modification of the Rectilinear Groove Method for the Analysis of Uniform Residual Stresses, *Exp Techniques*, **21**(6), 25-29.
69. Popelar CH, Barber T, and Groom J (1982), A Method for Determining Residual Stresses in Pipes, *J Pressure Vessel Tech*, **104**, 223-228.
70. Saxena A and Hudak SJ Jr. (1978), Review and Extension of Compliance Information for Common Crack Growth Specimens, *Int J Fract*, **14**(5), 453-467.
71. Schajer GS (1981), Application of Finite Element Calculations to Residual Stress Measurements, *J Eng Mat Tech*, **103**, 157-163.
72. Schajer GS (1988), Measurement of Non-Uniform Residual Stresses Using the Hole-Drilling Method, *J Eng Mat Tech*, **110**, 338-349.
73. Schindler HJ (1993), Weight Functions for Deep Cracks and High Stress Gradients, *Advances in Fracture Resistance and Structural Integrity*, Panasyuk VV et al. (eds), Pergamon Press, Oxford, UK.
74. Schwaighofer J (1964), Determination of Residual Stresses on the Surface of Structural Parts, *Exp Mech*, **4**(2), 54-56.
75. Soete W and VanCrombrugge R (1954), Determination of Residual Stresses Below the Surface, in *Residual Stresses in Metals and Metal Construction*, Osgood WR (ed), Reinhold Publishers, New York, NY, USA, **8**(1), 17-28.
76. Wu XR and Carlsson AJ (1991), *Weight Functions and Stress Intensity Factor Solutions*. Pergamon Press, Oxford, England.
77. Zuccarello B (1996), Optimization of Depth Increment Distribution in the Ring-Core Method, *J Strain Anal Eng Des*, **31**(4), 251-258.